

ASSESSING THE FEASIBILITY OF LOW-COST UNMANNED AERIAL VEHICLE
DATA COLLECTION AND AUTOMATIC TREE DETECTION TO DETERMINE
SILVICULTURE STAND STOCKING STATUS IN BC

by

Colin Langlois



Faculty of Natural Resources Management

Lakehead University

April 7, 2022

ASSESSING THE FEASIBILITY OF LOW-COST UNMANNED AERIAL VEHICLE
DATA COLLECTION AND AUTOMATIC TREE DETECTION TO DETERMINE
SILVICULTURE STAND STOCKING STATUS IN BC

by

Colin Langlois

An Undergraduate Thesis Submitted in Partial Fulfillment
of the Requirements for the Degree of
Honours Bachelor of Science in Forestry

Faculty of Natural Resources Management
Lakehead University

April 7, 2022

Ryan Wilkie
Major Advisor

Colin Filliter
Second Reader

LIBRARY RIGHTS STATEMENT

In presenting this thesis in partial fulfillment of the requirements for the Honours Bachelor of Science in Forestry degree at Lakehead University in Thunder Bay, I agree that the University will make it freely available for inspection.

This thesis is made available by my authority solely for the purpose of private study and research and may not be copied or reproduced in whole or in part (except as permitted by the Copyright Laws) without my written authority.

Date: _____ April 7, 2022 _____

A CAUTION TO THE READER

This Honours Bachelor of Science in Forestry thesis has been through a semi-formal process of review and comment by at least two faculty members. It is made available for loan by the Faculty of Natural Resources Management for the purpose of advancing the practice of professional and scientific forestry.

The reader should be aware that opinions and conclusions expressed in this document are those of the student and do not necessarily reflect the opinions of the thesis supervisor, the faculty or Lakehead University.

ABSTRACT

Langlois, C. 2022. Assessing the Feasibility of Low-Cost Unmanned Aerial Vehicle Data Collection and Automatic Tree Detection to Determine Silviculture Stand Stocking Status in BC. 84 pp.

Keywords: canopy height model, DAP, drone, individual tree detection, orthomosaic, pix4d, point cloud, RGB, silviculture, UAV.

The objective of this research was to evaluate the capabilities and limitations of low-cost UAV-collected silviculture data derived from Digital Aerial Photogrammetric point clouds. Four regenerating forest stands with a mix of planted spruce and lodgepole pine were surveyed using traditional ground plot surveys, aerial plot surveys, and aerial wall-to-wall surveys. A total of 22 systematic grid sampled ground plots were used as the baseline data to compare survey accuracy and efficiency of survey methods. Aerial survey imagery was processed using Pix4D software to produce orthomosaics and elevation data of each stand, which was used by a custom QGIS algorithm to identify stand stocking metrics. Compared to traditional ground plot surveys, the aerial plot survey method was determined to be 63% less accurate and 93% less efficient overall. The aerial wall-to-wall survey method was 63% less accurate and 942% more efficient overall. The reduced accuracy was found to be caused by a combination of equipment limitations and operational methods, including low point cloud density, GPS positional errors, camera angle, DTM creation, and ground sample distance (GSD). These major sources of error are examined and potential solutions are considered. Despite relatively low accuracies and variable efficiencies, the aerial methods require significantly lower fieldwork time, indicating potential cost savings in the near future.

CONTENTS

ABSTRACT	III
TABLES	VI
FIGURES	VIII
ACKNOWLEDGEMENTS	X
INTRODUCTION	1
OBJECTIVE	4
HYPOTHESES	4
LITERATURE REVIEW	5
UAV SURVEY METHODS	5
UAV FLIGHT LIMITATIONS	7
UAV SENSOR TYPES	8
STRUCTURE FROM MOTION AND POINT CLOUD DEVELOPMENT	10
METRIC CALCULATIONS FROM POINT CLOUDS	12
LIMITATIONS TO DAP POINT CLOUDS	14
DATA PROCESSING METHODS	17
STATISTICAL TESTING OF POINT CLOUD MEASUREMENTS	18
POLICY	21
MATERIALS AND METHODS	22
STUDY AREA	22
TRADITIONAL GROUND PLOT SURVEYS	23
UAV AERIAL DATA COLLECTION	25
AERIAL IMAGERY PROCESSING	28
RESULTS	34
GROUND PLOT AND AERIAL PLOT SURVEYS	34
GROUND PLOT AND WALL-TO-WALL SURVEYS	38
TIME AND EFFICIENCY	41
TIME AND EFFICIENCY COMPARISON	43

DISCUSSION	46
SOURCES OF LINEAR ERROR	48
SOURCES OF EXPONENTIAL ERROR	50
FUTURE DEVELOPMENT	54
BALANCING ACCURACY AND EFFICIENCY	55
CONCLUSION	58
LITERATURE CITED	59
APPENDIX I RAW CONIFER COUNT RESULTS FOR THE FOUR STANDS SURVEYED	70
APPENDIX II STAND A EXAMPLE OF 2D IMAGERY MATCHES DURING PIX4D PROCESSING	71
APPENDIX III COMPUTER PROCESSING SYSTEM INFORMATION	72

TABLES

Table	Page
Table 1. Common UAV image parameters used for wall-to-wall UAV surveys. Source: Puliti et al. (2019)	7
Table 2. Summary of statistical significance testing methods of similar studies.	20
Table 3. Basic attributes of the four stands selected for this study.	22
Table 4. Basic survey attributes of the four stands studied.	24
Table 5. DJI Mavic 2 Pro specifications. Source: DJI (2022).	26
Table 6. Aerial survey flight data.	27
Table 7. Conifer count data and accuracy comparison between ground plot survey and aerial plot survey methods	35
Table 8. Stand conifer data calculated from ground plot and aerial plot survey results.	36
Table 9. Sum of conifer count data from aerial wall-to-wall surveys.	38
Table 10. Conifer count data and accuracy comparison between ground plot survey and aerial wall-to-wall survey methods.	39
Table 11. Stand conifer data calculated from ground plot and aerial wall-to-wall survey results.	39
Table 12. Ground plot survey time summary.	41
Table 13. Aerial plot survey time summary.	42
Table 14. Aerial wall-to-wall survey time summary.	42

Table 15. Time and production rates for the three survey methods (ground plot, aerial plot, and aerial wall-to-wall).	43
Table 16. Net efficiency and accuracy comparison of the two aerial survey methods to the ground plot data which acts as the control data set.	44
Table 17. Work-hour efficiency and accuracy comparison for the three survey methods (ground plot, aerial plot, and aerial wall-to-wall).	45

FIGURES

Figure	Page
Figure 1. Aerial plot survey flight pattern used by Feduck et al. (2018).	6
Figure 2. SfM image processing workflow for dense point cloud development. Source: Iglhaut et al. (2019).	12
Figure 3. NGRDI, VARI, and GLI formulas as commonly used for automated RGB classification. Source: Goodbody et al. (2018).	17
Figure 4. Geographic location of the four stands studied. Source: Esri (2022).	23
Figure 5. Plot centres marked with spray painted "X". Image captured at 100 m AGL with the Hasselbad L1D-20c camera built in to the DJI Mavic Pro 2, pointed 90° towards the ground.	25
Figure 6. Manually flown flight path (green line) for stand A superimposed over the orthomosaic generated in Pix4D. Blue points along flight path represent photo locations.	27
Figure 7. Example of the point cloud mesh produced for Stand A in Pix4D.	28
Figure 8. Custom Tree Count algorithm work flow roughly based on Damer (2019). Developed using QGIS 3.20 Model Designer utilizing GDAL, GRASS, and SAGA Next Gen tools.	30
Figure 9. Stand A, plot 6 WS conifer output. (A) = Original orthomosaic, (B) = VARI layer clipped to plot area, (C) = CHM hillshade, (D) = CHM	

topography set to 0.1m intervals superimposed on the original orthomosaic.	32
Figure 10. Stand A (5.7 ha) aerial survey conifer outputs atop the orthomosaic layer. (A) = Total conifers, (B) = WS conifers, (C) = Total FG conifers, (D) = WS FG conifers.	33
Figure 11. Scatterplots of the aerial and ground surveyed plot data (y-axis) versus the field plot data (x-axis).	37
Figure 12. Scatterplots of the surveyed wall-to-wall & ground plot results (y-axis) versus the field plot data (x-axis).	40
Figure 13. CHM contours showing a blind spot example with conifer height errors.	49
Figure 14. Low resolution point cloud mesh showing poorly defined conifer clump.	49
Figure 15. Clumped Lodgepole pine growing below/adjacent to a central dominant stem.	51
Figure 16. An undetected spruce tree that was 20 cm wide showing relative pixel size.	53
Figure 17. Relative point cloud densities, 3D reconstruction details, and height estimation for a cluster of spruce trees. Source: Castilla et al. (2020).	57

ACKNOWLEDGEMENTS

I would like to thank my major advisor, Ryan Wilkie for the overall thesis guidance and invaluable UAV-related input. Special thanks to my second reader, Colin Filliter and the SuavAir crew for collecting data and providing the necessary resources to make this thesis possible. Finally, I would like to thank Alex Bilyk for the remote sensing courses which built a foundation of knowledge that will be used throughout my career.

INTRODUCTION

In British Columbia (BC), all forestry on crown land is governed by the Forest and Range Practices Act (FRPA) (MFLNRORD 2018). Before forestry activities can take place, license holders are required to prepare a forest stewardship plan (FSP) and obtain approval from the minister (FRPA 2002). Approved forest stewardship plans generally have a term of five to ten years and must conform to the objectives outlined in the FRPA (MFLNRORD 2018). As part of the obligations of a FSP, licence holders are to comply with post-harvest stand regeneration activities involving the establishment of a free growing stand (FRPA 2002; MFLNRORD 2018). These silvicultural obligations are measured by forest inventories required under the Forest Planning and Practices Regulation (FPPR) (MFLNRORD 2018).

Silviculture stocking standards outlined in a FSP ensure the long-term commercial timber supply in the forest (B.C. Ministry of Forests 2000). Guided by the Biogeoclimatic Ecosystem Classification (BEC), stocking standards are developed for density limits, tree spacing, preferred/acceptable species, free grow heights, and acceptable competition levels (MFLNRORD 2018). The licence holder assumes silvicultural liability and responsibility of a stand until it is declared free growing (FG) (B.C. Ministry of Forests 2000). According to FRPA (2002), a stand is considered FG if the commercially valuable trees are healthy and free from brush competition (based on stocking standards). Throughout the regeneration process, silviculture surveys are periodically conducted to ensure stocking standards are met (Goodbody et al. 2018). The

recurring surveys necessary to effectively manage a regenerating stand contribute to cumulative costs for license holders. A successful free grow survey is the final assessment of the stand, which relieves the licence holder of silvicultural responsibility once submitted to the provincial government (B.C. Ministry of Forests 2000).

In accordance with the BC Silviculture Surveys Procedures Manual, silviculture survey data is traditionally collected using 50m² circular ground plots by trained silviculture accredited surveyors at one plot per hectare (MFLNRORD 2020). The results from traditional ground surveys are sufficient for provincial reporting standards (MFLNRORD 2020), but can often result in low sample coverage of a given stand leading to unanticipated forest structures between sampling points. (Pouliot et al. 2002). Traditional silviculture surveys are often time consuming, costly, and accompanied by safety hazards (Pouliot et al. 2002; Liang et al. 2019; Mohan et al. 2017; Zhang et al. 2016; Chen et al. 2021; Chen et al. 2017). Similarly, the sampling intensity is often not high enough to accurately represent detailed spatial coverage in a stand (Goodbody et al. 2018; Pouliot et al. 2002). These factors become more significant as stand size increases (Liang et al. 2019; Röder et al. 2018; Chen et al. 2017). As a result of the time and cost of surveys, the frequency of silviculture surveys are operationally minimized (Pouliot et al. 2002; Mohan et al. 2017; Zhang et al. 2016). Infrequently conducted silviculture surveys can result in the progression of pests, disease, and undesired competition growth. Without early intervention, this results in significant crop tree mortality which increases regeneration costs through fill planting and/or brushing activities, and extends the time it takes for the stand to reach FG status.

The efficacy of sustainable forest management decisions are limited to the quality and quantity of data collected in the field (Puliti et al. 2019; MFLNRORD 2020; Pouliot et al. 2002; Haddow et al. 2000; Chen et al. 2021; Reid et al. 2019). Rapidly advancing unmanned aerial vehicle (UAV) technology is allowing more field data to be collected and processed than once thought possible (Mohan et al. 2017; Liang et al. 2019). The term “UAV” is synonymous with more modern terminology including “drone”, “unmanned aerial system (UAS)”, “remotely piloted aircraft system (RPAS)”, and “remotely piloted aircraft (RPA)”. Through the pursuit of new survey opportunities made available by UAV technology, the tools available to foresters will continually improve to allow for better management decisions (Goodbody et al. 2018; Puliti et al. 2019; Reid et al. 2019; Tang and Shao 2015). The emerging ability to collect and process high resolution multi-purpose data over entire stands will contribute to significant advancements in surveying methods (Mohan et al. 2017; Pouliot et al. 2002). Preliminary research suggests that UAV-collected data enables time savings of up to 2/3, and cost savings of up to 1/3 of traditional forest stand ground collected data (Röder et al. 2018) and likely to improve with future, technological or methodological advances.

However, the cost and portability of advanced UAV systems are limiting factors within the forest industry today (Vepakomma et al. 2015; Feduck et al. 2018; Röder et al. 2018; Zhang et al. 2016; Chen et al. 2017; Hird et al. 2017; Castilla et al. 2020). A potential solution to these current limiting factors is to identify the capabilities of Digital Aerial Photogrammetric (DAP) point clouds derived from UAV-collected red-green-blue (RGB) imagery (Goodbody et al. 2018). This relatively simple and cost-effective alternative has the potential to produce high accuracy silviculture outputs using

consumer-grade UAVs (Pouliot et al. 2002; Chen et al. 2017; Hird et al. 2017; Goodbody et al. 2018; Feduck et al. 2018; Castilla et al. 2020).

OBJECTIVE

The primary objective of this research is to evaluate the capabilities and limitations of low-cost UAV-collected silviculture data. The secondary objective is to compare the accuracy and costs of UAV survey methods compared to traditional ground surveys. The findings of this research intended to identify opportunities for licensees and contractors to improve efficiencies while improving data collection quality with the use of UAVs.

HYPOTHESES

This study includes a linear workflow addressing the following three hypotheses;

H₁: Total, well-spaced (WS), and FG conifer counts can be automatically detected using DAP point cloud processing algorithms.

H₂: There will be no significant difference (p -value < 0.1) between the total stem counts of the ground plot surveys compared to those of the UAV surveys.

H₃: If *H₂* is proven to be true, then aerial data collection is more efficient than ground surveys.

LITERATURE REVIEW

UAV SURVEY METHODS

To efficiently collect silviculture data, traditional ground surveys commonly use a systematic grid survey sampling method in stands. A standard 50m² sample plot per hectare results in a plot multiplier of 200, allowing minor human error, bias, or spatial variation to have a multiplied effect on final values (Pouliot et al. 2002; Asner et al. 2015). Emerging UAV technology reduces or eliminates the need for sample plots by collecting data for an entire stand (Tang and Shao 2015; Goodbody et al. 2018; Gallardo-Salazar and Pompa-García 2020; Hartley et al. 2020). Wall-to-wall surveys are common with UAV systems due to the ease of data collection, low flight costs, and wide range of spatial and temporal metrics (Zhang et al. 2016; Mohan et al. 2017; Goodbody et al. 2018; Reid et al. 2019). This survey method can collect high quality data at an estimated coverage rate of 36.9 ha/h (Feduck et al. 2018).

A different approach by Hird et al. (2017), Reid et al. (2019) and Feduck et al. (2018) uses sample-based UAV data collection, claiming wall-to-wall UAV silviculture data collection and processing is excessively time consuming. Since spatial resolution increases as altitude and flight speed decreases, high quality (<20 cm resolution) sample plots can be achieved in 1/5 of the time required for a wall-to-wall survey (Fernandez-Guisuraga et al. 2018; Feduck et al. 2018). Similar studies such as Zhang et al. (2016) achieved spatial resolutions of up to 5 cm, while Feduck et al. (2018) and Castilla et al. (2020) achieved millimetric spatial resolution using RGB imagery. A 16 MP Nikon

Coolpix camera flown at 15 m above ground level (AGL) was used by Feduck et al. (2018), and a Mavic Pro with the FC220 camera flown at 5 m AGL was used by Castilla et al. (2020). Figure 1 shows the aerial plot survey method used to achieve sub-centimeter spatial resolution.

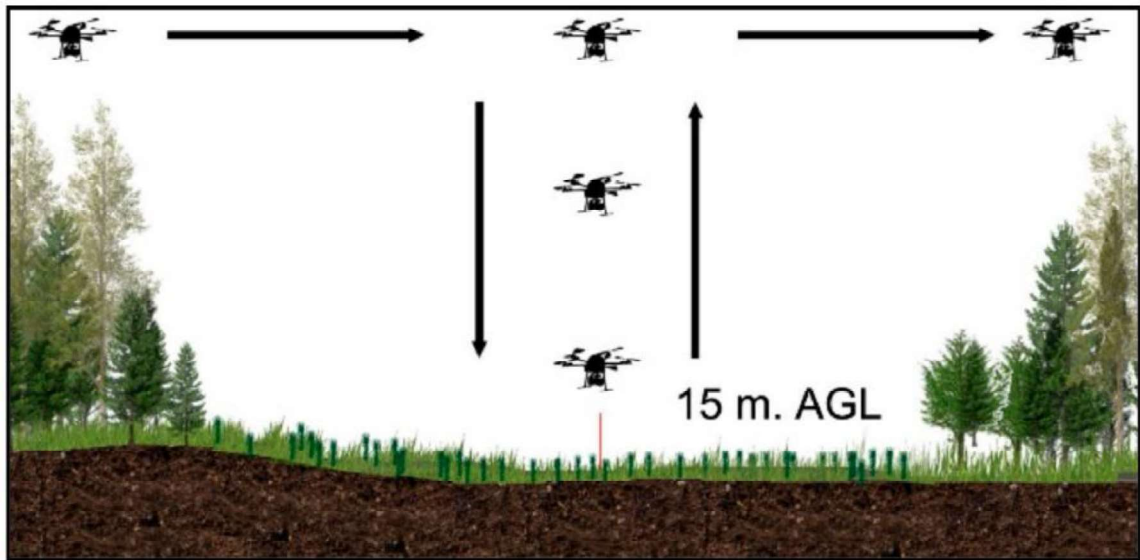


Figure 1. Aerial plot survey flight pattern used by Feduck et al. (2018).

UAV flight parameters varied slightly across similar studies. Typical wall-to-wall parameters closely resemble those in Table 1. For best wall-to-wall survey accuracy, double-grid flight patterns are created using flight planning software such as Map Pilot (Carr and Snyder 2018; Hartley et al. 2020), Pix4D Capture (Roder et al. 2018) and Mission Planner (Chen et al. 2017). Although flight planning software allows for consistent data collection, many are not capable of executing the flight with active collision avoidance. For flights in close proximity to the forest canopy or terrain, it is often preferential to conduct manual flight missions. Image parameters for aerial sample

plot surveys used in Hird et al. (2017) and Feduck et al. (2018) were similar to those in Table 1 with the exception of lower flight altitudes (15m to 75m), and reduced ground sampling distance (GSD) ranging between 0.3cm and 1.6cm.

Table 1. Common UAV image parameters used for wall-to-wall UAV surveys. Source: Puliti et al. (2019)

Parameter	Value
Flight altitude	110 m
Ground sampling distance	3 cm
Forward overlap	90%
Side overlap	80%
Flight speed	5 m sec

Although recent studies indicate successful results and potential industrial opportunities, there is no evidence of UAV survey adoption within the industry to date. To successfully implement UAV surveys in the forest industry, further research is needed to identify consistent point cloud metrics and develop resilient flight methods and processing workflows (Hird et al. 2017; Mohan et al. 2017; Röder et al. 2018; Feduck et al. 2018).

UAV FLIGHT LIMITATIONS

Unlike traditional ground surveys, UAVs have considerable limiting factors that can affect the success of a survey. Although relatively simple to operate, pilots of UAVs

(also known as RPAS) >250 g must be certified by Transport Canada. RPAS pilot certificates range from basic to advanced, both requiring online training and testing, with additional flight tests for the advanced certificate (Transport Canada 2020). UAV flights are limited by battery capacity affecting flight times (Goodbody et al. 2018) and meteorological factors such as wind speed, precipitation, and visibility. According to Transport Canada (2020), all RPAS must be operated within visual line of sight at all times, however operations beyond visual line of sight (BVLOS) can be authorized for specific purposes. To take full advantage of the potential efficiency of UAV surveys, BVLOS operations will likely be required (Goodbody et al. 2018; Nitoslawski et al. 2021). The combination of the mentioned UAV limitations do not significantly affect the potential practicality of UAV silviculture surveys. They do however add to the complexity of the process.

UAV SENSOR TYPES

Modern UAVs are capable of operating with various sensor types which are often interchangeable to suit survey objectives (Fernandez-Guisuraga et al. 2018). Sensors used for remote sensing commonly include passive RGB cameras, multispectral, and active LiDAR sensors (Goodbody et al. 2017; Nitoslawski et al. 2021). Currently, the most common sensors used for silviculture surveys are digital RGB cameras (Hird et al. 2017; Fernandez-Guisuraga et al. 2018; Dainelli et al. 2021). This is predominantly

because consumer-grade UAVs have become simple to operate, affordable, and highly portable (Mohan et al. 2017; Hird et al. 2017; Feduck et al. 2018; Liang et al. 2019).

The most significant drawback with DAP point clouds from RGB imagery is the highly variable GSD dependent on altitude and camera parameters. This variation can affect the accuracy of data throughout a forest stand, which affects the types of metrics that can be derived from the data. Despite a relatively low DAP point cloud GSD of < 1 cm, airborne laser scanning (ALS) sensors are generally more accurate and more efficient over large areas (Castilla et al. 2020; Mohan et al. 2017). As consumer grade cameras and image processing algorithms improve, RGB data collection will be increasingly suitable for complex forest structure surveys (Dvořák et al. 2015; Hird et al. 2017; Liang et al. 2019).

ALS uses active LiDAR to produce high resolution point clouds capable of modeling complex vegetation structures (Chen et al. 2017; Goodbody et al. 2017). The laser pulses penetrate through forest canopies and dense brush, allowing complete vertical forest structures to be captured and classified (Chen et al. 2017; Hird et al. 2017; Hartley et al. 2020). Unlike DAP point clouds which struggle to accurately represent areas with high vegetation cover and stand densities, ALS point clouds are relatively unaffected by these factors (Goodbody et al. 2018). However, they can be very noisy when data is collected during windy conditions due to swaying tree tops (Castilla et al. 2020). Although this advanced system can produce highly accurate forest models for a wide range of products (Goodbody et al. 2017), these sensors are rarely used in the forest industry for stand-level surveys (Goodbody et al. 2017; Röder et al. 2018). ALS-mounted UAV systems are among the most costly data collection methods and require

technical data management expertise (Zhang et al. 2016; Chen et al. 2017; Goodbody et al. 2017; Feduck et al. 2018).

UAV-mounted hyperspectral and multispectral sensors such as the DJI Phantom 4 Multispectral (P4M) acquire a wide range of reflectance data beyond the visual RGB bands (Gallardo-Salazar and Pompa-García 2020). These sensors allow for further metrics to be collected including biochemical and biophysical attributes to identify individual species and determine forest health (King 2000; Zhang et al. 2016; Goodbody et al. 2018; Saarinen et al. 2018; Iglhaut et al. 2019; Gallardo-Salazar and Pompa-García 2020). Some limitations of RGB individual tree detection can be resolved by multispectral delineation of the subtle phenotypic reflectance differences within clumps of trees (Asner et al. 2015; Goodbody et al. 2018). While simple RGB imagery often requires semi-automated tree detection methods (Goodbody et al. 2018; Nitoslawski et al. 2021), the collection of high resolution multispectral imagery may allow for fully-automated tree detection methods (Asner et al. 2015; Goodbody et al. 2018).

STRUCTURE FROM MOTION AND POINT CLOUD DEVELOPMENT

Recently developed processing software is able to produce three-dimensional point clouds by automatically stitching and triangulating a series of overlapping photographs (Chen et al. 2017; Hird et al. 2017; Mohan et al. 2017; Goldbergs et al. 2018; Iglhaut et al. 2019; Castilla et al. 2020; Hartley et al. 2020). This process, known as structure from motion (SfM), compares the changes in aspect of photographed

features and GPS data to calculate relative elevation (Mohan et al. 2017; Goldbergs et al. 2018; Castilla et al. 2020). For increased accuracy, optional ground control points (GCPs) positioned by surveyors ensure GPS data is referenced to a local confirmed point (Mohan et al. 2017; Nevalainen et al. 2017; Chen et al. 2017; Goldbergs et al. 2018; Goodbody et al. 2018; Puliti et al. 2019). SfM allows large amounts of aerial imagery data to be efficiently compiled into digital outputs (Mohan et al. 2017). Common SfM processing software used for individual tree detection includes paid software such as Agisoft Photoscan (Vepakomma et al. 2015; Mohan et al. 2017; Nevalainen et al. 2017; Hird et al. 2017; Chen et al. 2017; Liu et al. 2018; Roder et al. 2018; Goldbergs et al. 2018; Puliti et al. 2019; Castilla et al. 2020; Chen et al. 2021; Dainelli et al. 2021), Pix4D Mapper (Zhang et al. 2016; Goodbody et al. 2017; Goodbody et al. 2018; Carr and Slyder 2018; Liu et al. 2018; Fernandez-Guisuraga et al. 2018; Hartley et al. 2020; Chadwick et al. 2020; Dainelli et al. 2021), and DroneDeploy (Dainelli et al. 2021). Alternatively, free open source software such as OpenDroneMap (ODM) can be used (Gallardo-Salazar and Pompa-García 2020). All data collected for this study was processed using Pix4D Mapper software.

These software packages produce common geomatics outputs including orthomosaics, point clouds, digital surface models (DSMs), and digital terrain models (DTMs) used for data analytics (Mohan et al. 2017; Nevalainen et al. 2017; Goodbody et al. 2017; Puliti et al. 2019; Hartley et al. 2020; Gallardo-Salazar and Pompa-García 2020; Dainelli et al. 2021). A DSM represents the surface elevation of all features including trees, brush, and topography. A DTM represents the topographic elevation

only, omitting all other features such as trees and brush. The SfM image processing workflow for dense point clouds used in this study is shown in (Figure 2).

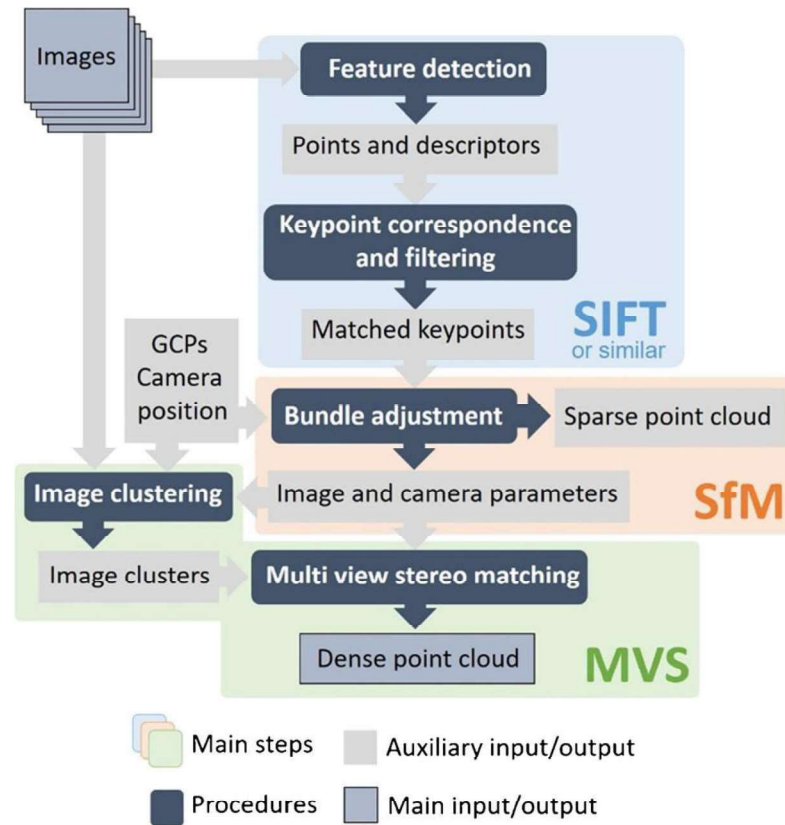


Figure 2. SfM image processing workflow for dense point cloud development. Source: Iglhaut et al. (2019).

METRIC CALCULATIONS FROM POINT CLOUDS

The two most common metrics derived from DAP point clouds are individual tree height data derived from SfM elevation data (Pouliot et al. 2002; Goodbody et al. 2017; Hartley et al. 2020), and tree count data derived from reflectance values

(optionally assisted by SfM elevation data) (Pouliot et al. 2002; Chen et al. 2021).

Further calculated metrics include stem density values for all conifers, WS conifers, and FG conifers, along with overall canopy closure, brush density/height, crown size, biomass volume, stand health indices, species composition, and ecosystem components (Pitt et al. 2000; Zhang et al. 2016; Mohan et al. 2017; Goodbody et al. 2018).

Individual tree height values are generally determined from a canopy height model (CHM), calculated by subtracting the DTM from the DSM to output height above ground (Puliti et al. 2019; Hartley et al. 2020). Inconsistencies between the two input models are often encountered in regenerating forest stands due relatively short vegetation heights and high stand densities, resulting in CHM errors (Goodbody et al. 2017; Goodbody et al. 2018; Hartley et al. 2020). To eliminate this error, Goodbody et al. (2017) suggests using ALS-derived DTM data in conjunction with DAP-derived DSM data to produce the CHM. Other minor height errors have been noted in data collected without the use of GCPs, causing height errors due to poorly calibrated SfM GPS data (Puliti et al. 2019). Relying solely on the UAV GPS location data can result in unreliably low location accuracy (5 to 20 m error), which can be degraded further by terrain obstructions and GPS satellite availability as experienced by Goldbergs et al. (2018). A combination of these factors can contribute to significant SfM elevation errors.

Early studies on DAP point cloud metrics proved accurate vegetation heights could be attained while using Trimble GCPs with sub-meter accuracy (Hird et al. 2017). As technology and processing power has improved, accurate individual tree detection has been proven to various extents. Castilla et al. (2020) used practical wall-to-wall

UAV surveys with a GSD < 0.5 cm and the use of GCPs to identify tree heights of planted conifer trees >30 cm tall (%RMSE = 40%, $R^2 = 0.63$). In this case, the DAP point cloud height metrics were more accurate than ALS data. An acceptable range of height error will vary depending on desired metrics. The focus of this study is the determination of silviculture status based on stocking and heights, which would require the range of tree height error to not be more than the difference between FG height and determined tree heights (e.g. FG height = 1 m, determined tree height = 2 m, and the range of error = +/- 0.5 m, proving the tree is FG). Any measured tree height within the range of error of FG height will negatively affect the confidence level of the final output. Limited by current technology, the measurement of trees under 30 cm is likely not practically possible using DAP point clouds alone (Castilla et al. 2020) but could still be useful in other silvicultural monitoring outside the scope of this thesis. Further research and development for fine-scale detection is required to address this limitation (Zhang et al. 2016).

LIMITATIONS TO DAP POINT CLOUDS

The simplicity of using consumer grade RGB data is associated with several important limitations to consider. DAP point cloud density can be considerably lower than LiDAR point clouds (Chen et al. 2017; Hird et al 2017). As a result, complicated forest structures such as competing vegetation or identifying single stems in clumped trees contributes to significant errors (Pouliot et al. 2002; Liang et al. 2019; Castilla et

al. 2020). The development of point clouds from RGB imagery is also known to incorporate distortions and mosaicked objects during the stitching process (Feduck et al. 2018). For these reasons, some studies suggest RGB point clouds are only practical as an alternative survey method for small stands with homogeneous stand structure and minimal competition (Röder et al. 2018; Mohan et al. 2017; Hird et al 2017). It is possible to produce high density DAP point clouds by collecting more imagery at lower altitudes and using cross-hatched survey methods (Zhang et al. 2016; Feduck et al. 2018; Fromm et al. 2019; Dainelli et al. 2021), but the process is very time consuming and not practical for larger stands (Mohan et al. 2017). From a data management perspective, the volume of high resolution RGB data collected across large stands has proven to be difficult (Fernandez-Guisuraga et al. 2018). The increasing number of images with increased sampling exponentially increases computational times post-flight.

Aside from point cloud accuracy, RGB imagery is also highly susceptible to radiometric inconsistencies caused by variable atmospheric conditions (Goodbody et al. 2018; Dvořák et al. 2015; Mohan et al. 2017; Feduck et al. 2018). Windy conditions also create point cloud errors caused by vegetation swaying while data is being collected, resulting in adjacent ‘ghost trees’ to appear (Iglhaut et al. 2019; Castilla et al. 2020). Data collected during windy conditions may result in a proportion of tree count false positives, but is predominantly expected to only affect outlier trees with heights above the stand average. The extent of this error can be reduced by increasing image overlap (Iglhaut et al. 2019). Similarly, poor lighting or the presence of shadows poorly affects the data due to the limited spectral range of RGB sensors (Dvořák et al. 2015; Zhang et al. 2016).

The accuracy and type of metrics that can be achieved in a stand is often limited by the species composition and structure found within (Goodbody et al. 2018). Generally in regenerating stands, DAP stand stocking and tree count detection accuracy increases as tree age decreases since younger trees occupy less area, and are therefore easier to delineate. This correlation was observed by Feduck et al. (2018), achieving 96% tree detection accuracy of conifer seedlings less than five years old using a high resolution RGB orthomosaic (with no height data). Minor errors in DSM and DTM data make tree height detection of small conifers (< 30 cm) unreliable (Castilla et al. 2020). In contrast, DAP tree height detection accuracy generally increases as tree age increases since larger trees have more surface area to produce more defined point cloud features. Unfortunately, larger trees cannot be delineated by reflectance value as easily due to spatial proximity, resulting in less accurate stand stocking and tree count detection for complex stand structures (Castilla et al. 2020).

In an effort to account for the above limitations, the work flows described in Feduck et al. (2018), Chadwick et al. (2020), and Castilla et al. (2020) recommend stands be surveyed during seasonal leaf-off conditions when coniferous trees are spectrally distinct against the brush and ground. Tree detection accuracy is greatest at this time, and results during other seasons are expected to be significantly lower.

DATA PROCESSING METHODS

Individual tree detection (ITD) using DAP point clouds commonly use automated classification algorithms within geographic information system (GIS) software such as QGIS (Nevalainen et al. 2017) or ArcGIS Pro (Carr and Snyder 2018). To delineate coniferous trees, imagery is classified based on reflectance value. For RGB data, visible vegetation indices such as the Visible Atmospherically Resistant Index (VARI), the Normalized Green Red Difference Index (NGRDI), and the Green Leaf Index (GLI) are effectively used (Figure 3) (Goodbody et al. 2018). Some studies such as Nevalainen et al. (2017) suggest multispectral data collection can lead to more accurate automated detection due to the increase in spectral bands. Tree height and structure is automatically determined using CHM values to identify tree tops. Although this data is not required for simple tree count tasks, it is often helpful to identify the precise tree stem locations.

$$\text{NGRDI} = \frac{R_g - R_r}{R_g + R_r}$$
$$\text{VARI} = \frac{R_g - R_r}{R_g + R_r - R_b}$$
$$\text{GLI} = \frac{2 R_g - R_r - R_b}{2 R_g + R_r + R_b}$$

Figure 3. NGRDI, VARI, and GLI formulas as commonly used for automated RGB classification. Source: Goodbody et al. (2018).

The accuracy of ITD algorithms can vary widely as they are dependent on reflectance values, point density, tree density, and forest structure (Mohan et al. 2017; Goodbody et al. 2018), along with many external factors. As a result, this automated process is currently limited to simple stand structures with homogenous species. The often large amount of data collected for wall-to-wall surveys requires expensive, powerful computers for processing and can be excessively time consuming (Feduck et al. 2018).

An alternative ITD method is the process of manually counting and measuring point cloud data using visual observation and measurement (Roder et al. 2018; Chen et al. 2021). Tree tops and heights can be identified using a combined point cloud mesh with the RGB orthomosaic within SfM or GIS software. This method is often more accurate than automated ITD methods, however it is significantly more time consuming (Roder et al. 2018; Chen et al. 2021). As opposed to automated methods which use (often) inaccurately smooth DTMs, manually measuring tree heights the raw point cloud mesh ensure minimal digital data manipulation (Chen et al. 2021).

STATISTICAL TESTING OF POINT CLOUD MEASUREMENTS

Depending on metrics measured, results of similar studies underwent several statistical tests to determine accuracy significance (Table 2). ITD accuracy determination included tests such as false positive, false negative, and true positive comparisons, one-way ANOVAs, and scatter plot regression. ITD studies in mature

conifer stands and in regenerating stands with simple structures show relatively high and consistent ITD accuracy. Root-mean-square-error (RMSE) tests determined the accuracy of tree height, crown area, and diameter measurements. Results from these metrics generally show variable and unreliable accuracies.

Table 2. Summary of statistical significance testing methods of similar studies.

Literature	Stand Attributes	UAV Data Collected/Measured	Output(s) Analysed	Tree Detection Method	Overall Accuracy	Validation Method(s)	Statistical Testing Method(s)
Mohan et al. 2017	32 ha of mature, open canopy mixed conifer in Wyoming	Orthomosaic and CHM derived from RGB imagery and SfM	ITD accuracy	Local Maximum (LM) algorithm	86%	Tree count/GPS data from 30 random 400m ² ground plots	False positive, false negative, true positive comparison
Chen et al. 2021	3 rectangular plots 900m ² each, in a 30 year old Chinese Fir plantation	Orthomosaic and CHM derived from RGB imagery and SfM	ITD accuracy	Local Maximum (LM) algorithm	85%	Complete enumeration of tree count/GPS data from ground	False positive, false negative, true positive comparison, One-way ANOVA
Feduck et al. 2018	20.3 ha training site, and 3.3 ha test site with 3–4 year old planted lodgepole pine and white spruce	Orthomosaic and CHM derived from RGB/RE imagery and SfM	ITD accuracy	Conifer seedling delineation using machine learning and training sites	96% (RGB only) 97% (RE only) 97% (RGB & RE)	Tree count/GPS data from 10 circular field plots, 50m ² each	Direct sample area regression between reference seedlings and classified seedlings
Castilla et al. 2020	3 separate regenerating seismic line sites in Alberta, each with two 100m ² belt plots	Orthomosaic and CHM derived from RGB imagery and SfM	Conifer height accuracy	CHM-derived equation	Seedlings < 30 cm: No relationship Seedlings > 30 cm: RMSE = 24 cm, bias = -11 cm, R ² = 0.63, n = 48	Complete enumeration of tree count/GPS data and tree heights from ground	RMSE and regression between reference seedlings and classified seedlings
Vepakomma et al. 2015	0.4 ha surveyed area within a 2 ha white spruce plantation in Quebec, and 0.4 ha surveyed area within a 6 ha of loblolly pine saplings in Alberta	Orthomosaic and CHM derived from RGB imagery and SfM	ITD and height accuracy	Local Maximum (LM) algorithm	ITD: 98% Tree height: 90%	Tree count/GPS data and tree heights for 9 randomly selected trees, and four 8 m X 10 m plots in each study area from ground	Direct sample area comparison between reference seedlings and classified seedlings
Gallardo-Salazar and Pompa-García 2020	1.1 ha of a pine clonal seed orchard in Mexico	Orthomosaic and CHM derived from RGB and B/G/R/E/NIR imagery and SfM	ITD, height, area, and crown diameter accuracy	Local Maximum (LM) algorithm	ITD: 95% Height: RMSE = 0.36 m, bias = -5.46 x 10 ⁻⁵ m, r (p<0.001) = 0.97 Area: RMSE = 3.88 m ² , bias = 2.17 x 10 ⁻⁷ m ² , r (p<0.001) = 0.95 Crown Diameter: RMSE = 0.47 m, bias = -3.57 x 10 ⁻⁵ m, r (p<0.001) = 0.95	Complete enumeration of tree count, height, area, and crown diameter from ground	RMSE and regression between ground measured and automatically detected conifers
Pouliot et al. 2002	Ten 42x14 m subplots of 6 year old black spruce and jack pine in Sault Ste. Marie, Ontario	G/R/NIR imagery	ITD accuracy	Local Maximum (LM) algorithm	Detection Accuracy: 90% Delineation Accuracy: 17.9% error	Tree crown diameters and location data of inner 25 trees in each subplot from ground	Detection Accuracy: Direct tree count accuracy comparison Delineation Accuracy: RMSE (%) comparison

POLICY

For UAV silviculture surveys to be fully integrated into the forest industry, the policies must adapt to the technological changes. Several provinces including BC, Ontario, and Saskatchewan have integrated UAV data collection into some aspects of FG surveys (Reid et al. 2019; MFLNRORD 2020). Despite this, silviculture surveyors are still required to complete necessary ground truthing and stand measurements (MFLNRORD 2020). The regulations involving RPAS such as the process to conduct BVLOS operations must be simplified to accommodate the operational requirements of UAV surveying (Nitoslawski et al. 2021). UAV-collected data such as RGB point clouds are expected to be integrated into forestry audits and silviculture compliance inspections (Goodbody et al. 2018). The complete enumeration of total stems in an opening determined by wall-to-wall surveys is expected to be a valuable metric in the near future (MFLNRORD 2020). It is expected that UAV-mounted LiDAR and multispectral sensors will likely replace a significant amount of silviculture ground surveys, and the policies are expected to change to accommodate this (Feduck et al. 2018; MFLNRORD 2020).

MATERIALS AND METHODS

STUDY AREA

A total of four stands within the 100 Mile House Resource District of the Cariboo Region of BC were chosen for this study (Table 3). Similar to Röder et al. (2018), Mohan et al. (2017), and Hird et al (2017), stands were selected based on their similar planted species (lodgepole pine (*Pinus contorta* D.) and spruce (*Picea* M.), and their relatively small net area to accommodate operational constraints. The geographic location of each stand is represented in Figure 4. All field data was collected between October 9, 2021 and October 14, 2021.

Table 3. Basic attributes of the four stands selected for this study.

Stand ID	Stand Size (ha)	BEC Zone	Minimum Elevation (m)	Maximum Elevation (m)
A	5.7	SBPS/mk	980	1025
B	2.8	ICH/mk	1020	1040
C	5.3	ESSF/wk	1300	1350
D	6.3	ESSF/wk	1325	1375

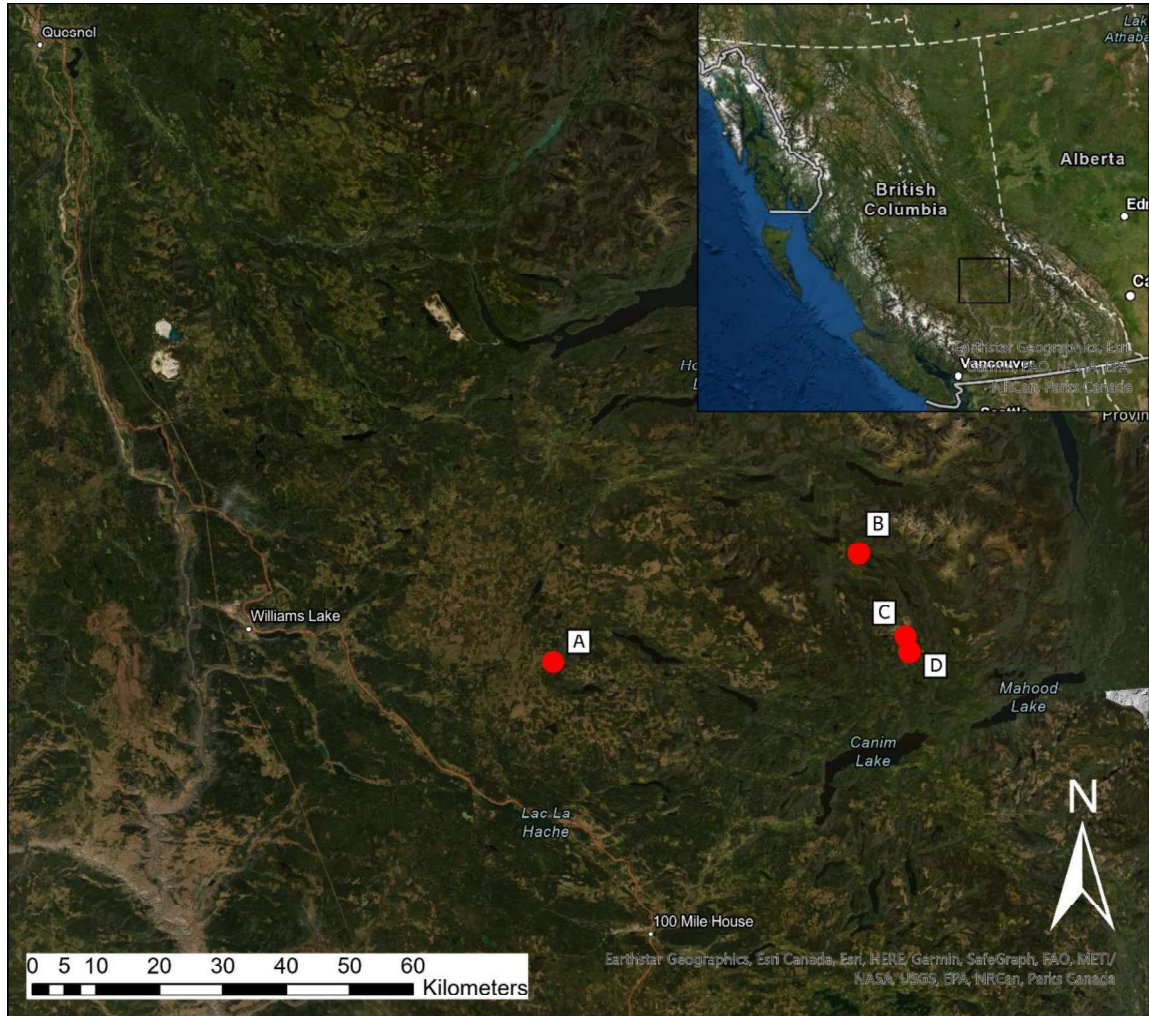


Figure 4. Geographic location of the four stands studied. Source: Esri (2022).

TRADITIONAL GROUND PLOT SURVEYS

As part of the planning process, a systematic grid sampling method was used to determine plot locations throughout each stand. The traditional ground plot survey was then conducted in each stand (Table 4) using 3.99 m radius plots consistent with the methods outlined in the *Silviculture Surveys Procedures Manual* (MFLNRORD 2020). In addition to marking plot centres with ribbon, each plot centre was marked on the

ground with a red “X” spray painted 1 m in diameter (Figure 5). All conifer ground survey data (total conifers, WS conifers, and FG conifers) was recorded and automatically compiled using SNAP data collection software on Apple iPads. For the purpose of this study, the distance between conifer piths must meet or exceed the minimum inter tree distance to be considered WS. To be considered FG, conifers must be WS and ≥ 0.8 m tall. Due to the unknown and likely poor ability for DAP point clouds to model young deciduous trees, it is assumed that there were no other limiting factors to be considered FG.

Table 4. Basic survey attributes of the four stands studied.

Stand ID	Minimum Inter Tree Distance (m)	Stand Size (ha)	Number of Plots	Age of Planted Stock (yrs)
A	2.0	5.7	6	11
B	1.6	2.8	5	14
C	2.0	5.3	5	14
D	2.0	6.3	6	12



Figure 5. Plot centres marked with spray painted "X". Image captured at 100 m AGL with the Hasselbad L1D-20c camera built in to the DJI Mavic Pro 2, pointed 90° towards the ground.

UAV AERIAL DATA COLLECTION

Aerial data was collected using a DJI Mavic 2 (Table 5) flown manually with the camera pointed at a 90° angle towards the ground, with an automatic 2-second shutter interval. Automated double-grid mapping missions similar to those used in Roder et al. (2018) were the preferred flight method, but it was more practical to fly manual missions (Figure 6) due to the risk of collision with variable terrain and obstacles. As discussed, the quality of data increases as flight altitude decreases, so attempts were made to fly as low as consistently possible in each stand (Table 6). However, residual mature aspen

scattered throughout the stands restricted flights to altitudes higher than the desired 20 m altitude. Based on the altitude and shutter interval, the optimal flight speed was determined to be 8 m/s to produce an image overlap of 70%. The flight speed varied slightly during flights as a result of manually flown surveys.

Table 5. DJI Mavic 2 Pro specifications. Source: DJI (2022).

DJI Mavic 2 Pro Feature	Specification
Weight w/ Battery (g)	907
Flight Time (min)	31
Maximum Speed (km/h)	72
Maximum Flight Distance (km)	18
Operating Temperature Range (°C)	-10 to 40
Horizontal GPS Accuracy (m)	3
Vertical GPS Accuracy (m)	5
RGB Camera Sensor	Hasselbad L1D-20c
Image Dimensions (px)	5472 × 3648
Field of View (°)	77
Sensor Type	1" CMOS

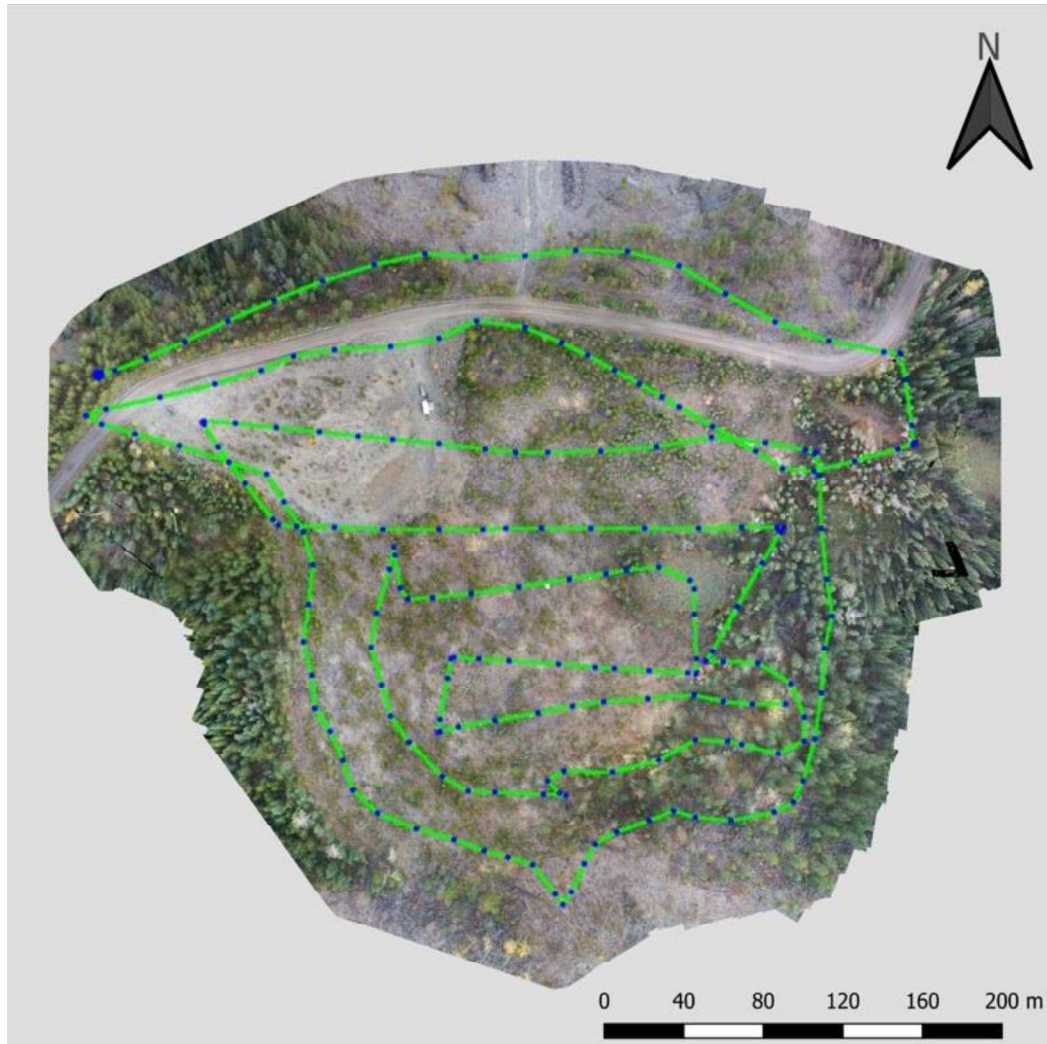


Figure 6. Manually flown flight path (green line) for stand A superimposed over the orthomosaic generated in Pix4D. Blue points along flight path represent photo locations.

Table 6. Aerial survey flight data.

Stand ID	Area (ha)	Altitude AGL (m)	# Aerial Images	Mean Orthomosaic Resolution (cm/px)	Point Density (per m ²)	Time of Day	Wx
A	5.7	100	204	2.54	1954.29	Morning	Overcast, no precipitation
B	2.8	130	90	3.31	846.95	Morning	Overcast, no precipitation
C	5.3	165	333	2.65	1797.84	Morning	Overcast, light snow
D	6.3	110	237	2.8	1488.47	Morning	Overcast, no precipitation

AERIAL IMAGERY PROCESSING

The aerial imagery for each stand was initially processed using Pix4D Mapper software to create a point cloud mesh (Figure 7), orthomosaic, DSM, and DTM layer. Using QGIS, the Visible Atmospheric Resistance Index (VARI) was calculated from the RGB bands of the orthomosaic to delineate conifer trees from other vegetation. A CHM was also calculated based on the DSM and DTM layer values.



Figure 7. Example of the point cloud mesh produced for Stand A in Pix4D.

The Tree Count algorithm for this study was developed in QGIS using the Graphical Modeller tool and a process based on Damer (2019). The complete Tree Count workflow is presented in Figure 8. The two required inputs are an indexed orthomosaic (VARI for RGB orthomosaics) clipped to the survey area and a full-size CHM. Based on index values, the algorithm isolates conifer trees, identifies conifer tree tops from the CHM, and assigns each tree top an ID and height value. To filter the conifers based on WS silviculture requirements, the algorithm optimizes the dataset by filtering conifers <2m apart horizontally, biased to tallest conifers. The algorithm outputs four shapefiles containing the total conifers, total WS conifers, total FG conifers, and total WS FG conifers. The complete tree counts are automatically compiled into a single Excel spreadsheet for data analysis.

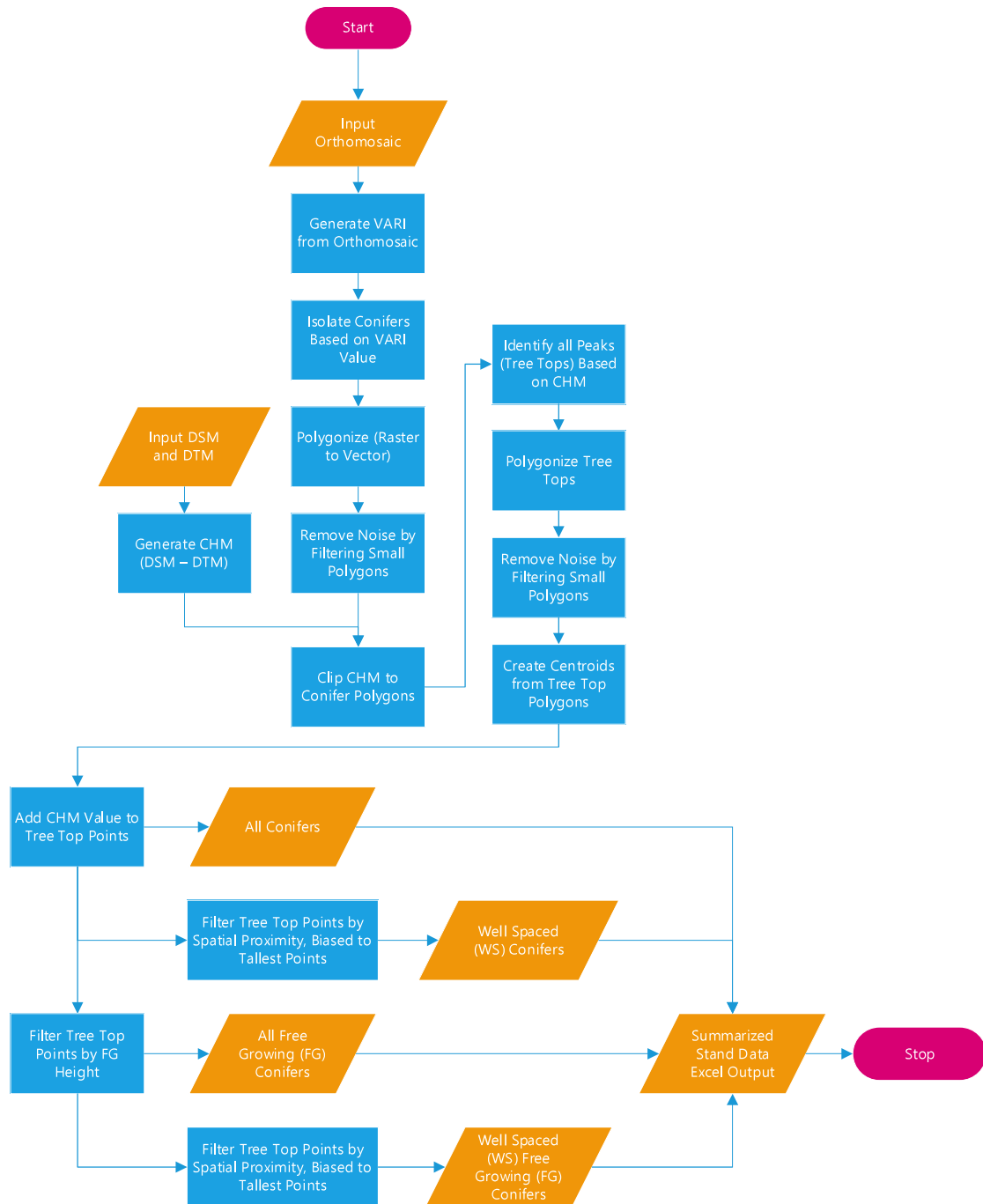


Figure 8. Custom Tree Count algorithm work flow roughly based on Damer (2019). Developed using QGIS 3.20 Model Designer utilizing GDAL, GRASS, and SAGA Next Gen tools.

Ground Plot Area Only

The precise plot centres for each survey were located from the orthomosaic and a 3.99 m buffer was added to represent the same area surveyed on the ground. The area outside the ground plots was clipped from the VARI layer. Using the clipped VARI and full-size CHM as inputs, the Tree Count algorithm calculates the various conifer outputs for the entire ground-sampled area. An example of the input layers and results are demonstrated in Figure 9. All species identification and field measurements collected during the ground plot surveys are assumed to be 100% accurate, with all conifers and deciduous trees in the sample area accounted for. Although proximity to deciduous trees can affect FG status of conifers, this aspect was excluded from this study as it is designed as a proof of concept. Further data analysis is required to determine detection reliability of deciduous trees in the future.

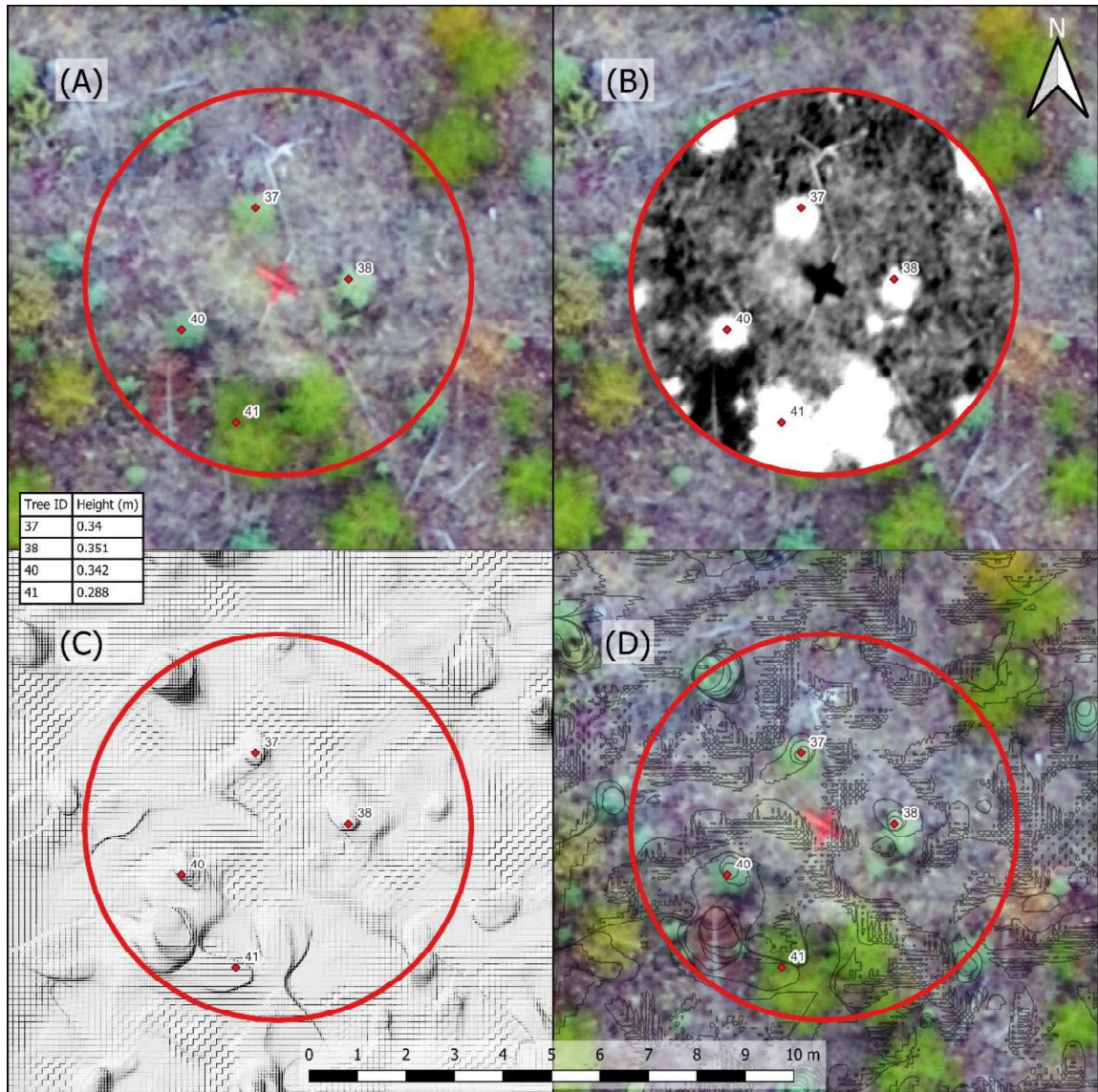


Figure 9. Stand A, plot 6 WS conifer output. (A) = Original orthomosaic, (B) = VARI layer clipped to plot area, (C) = CHM hillshade, (D) = CHM topography set to 0.1m intervals superimposed on the original orthomosaic.

Wall-to-Wall Stand Area

The VARI must be clipped to the extent of the stand area and input into the Tree Count algorithm along with the full-size CHM. The various conifer outputs for the entire

stand were calculated and visually inspected for accuracy. An example of the output results are represented in Figure 10.

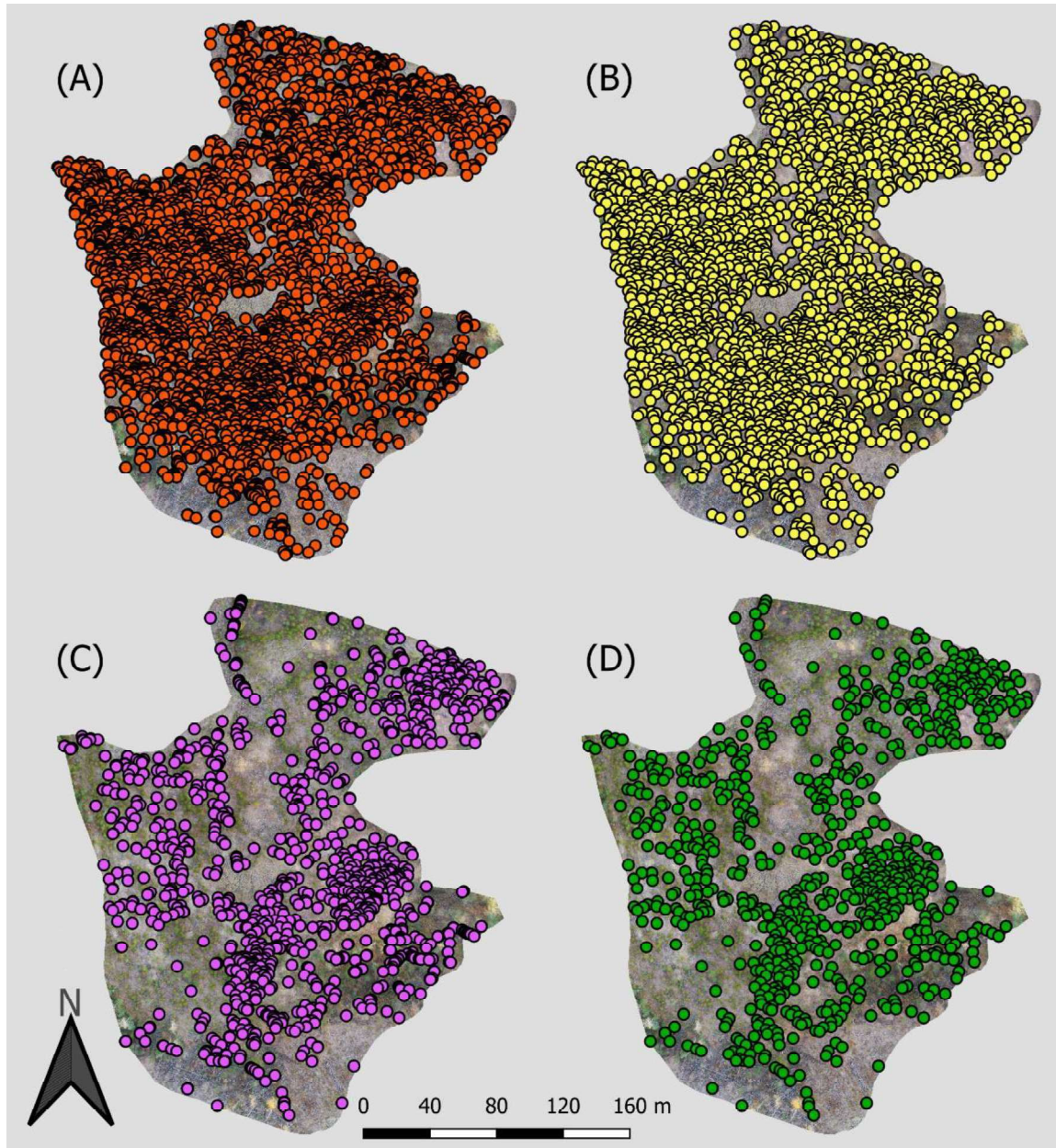


Figure 10. Stand A (5.7 ha) aerial survey conifer outputs atop the orthomosaic layer. (A) = Total conifers, (B) = WS conifers, (C) = Total FG conifers, (D) = WS FG conifers.

RESULTS

GROUND PLOT AND AERIAL PLOT SURVEYS

A total of 22 plots were surveyed in the four stands, producing accurate baseline counts for total conifers, WS conifers, and FG conifers in each plot. 256 conifers were counted in the 1,100 m² area surveyed on the ground. The Tree Count algorithm correctly identified 104 conifers within the same 1,100 m² ground plot survey area. Based on survey data in APPENDIX I, a summary of this data is represented in Table 7. A direct comparison between the baseline ground plot conifer counts and the aerial plot conifer counts indicate the aerial plot method underestimated all three categories of conifer counts (total, WS, and FG). The Total Conifers category of each stand ranged from 34% to 44% accuracy with a mean accuracy of 39%. The WS Conifers category ranged from 30% to 62% accuracy resulting in the highest mean accuracy of 41%. The FG Conifers category ranged from 9% to 46% accuracy with the lowest mean accuracy of 29%.

Table 7. Conifer count data and accuracy comparison between ground plot survey and aerial plot survey methods

Stand ID	Stand Sample Size (%)	Total Conifer			WS Conifer			FG Conifer		
		Ground Plot Survey Count	Aerial Plot Survey		Ground Plot Survey Count	Aerial Plot Survey		Ground Plot Survey Count	Aerial Plot Survey	
			Count	Accuracy		Count	Accuracy		Count	Accuracy
A	0.09%	106	47	44%	36	15	42%	35	3	9%
B	0.18%	32	11	34%	26	8	31%	19	6	32%
C	0.09%	65	28	43%	29	18	62%	26	12	46%
D	0.08%	53	18	34%	30	9	30%	16	5	31%
Total		256	104	39%	121	50	41%	96	26	29%

Following the procedures in the BC Silviculture Surveys Procedures Manual (MFLNRORD 2020), the ground plot and aerial plot survey data was used to determine the stems per hectare (SPH) and lower confidence limits (LCL) for all conifers, WS conifers, and FG conifers throughout each entire stand (Table 8). The target FG stocking for all stands was 1200 SPH with a minimum stocking of 700 SPH. With the LCL in consideration, the ground plot method can prove stands A and C are FG. Due to the mean SPH and LCL of stands B and D, these stands are considered not free growing (NFG). The same comparison can be made from the FG aerial plot method, showing all stands are considered NFG based on the mean SPH and LCL.

Table 8. Stand conifer data calculated from ground plot and aerial plot survey results.

Stand ID	Total Conifers				WS Conifers				FG Conifers			
	Ground Plot		Aerial Plot		Ground Plot		Aerial Plot		Ground Plot		Aerial Plot	
	Mean (SPH)	LCL (SPH)	Mean (SPH)	LCL (SPH)	Mean (SPH)	LCL (SPH)	Mean (SPH)	LCL (SPH)	Mean (SPH)	LCL (SPH)	Mean (SPH)	LCL (SPH)
A	3533	2002	1567	356	1200	1100	500	273	1167	1048	100	0
B	1280	821	440	99	1040	791	320	149	760	511	240	31
C	2600	1837	1120	571	1160	954	720	348	1040	898	480	309
D	1767	1081	600	159	1000	853	300	73	533	245	167	43
Mean	2295	1435	932	296	1100	925	460	211	875	676	247	96

The relationships between the aerial plot results and the ground plot results are represented in Figure 11 under two analyses. The conifer detection linear regression scatterplots demonstrates that the aerial plot surveys are not significantly correlated (p -value < 0.1) to the baseline ground plot surveys in any conifer count category (total, WS, and FG). The linear regression results indicate that the FG conifer count had the highest correlation between survey methods, while the total conifer count had the lowest correlation. If a significant correlation did exist between the two survey methods, the linear regression aerial plot data would show a similar slope and y-intercept as the ground plot data as a result of less conifer count variation in each plot.

The exponential relationship of conifer count/plot scatterplots demonstrates that in all conifer count categories (total, WS, and FG), the aerial plot survey conifer count error increases exponentially as actual conifer count increases.

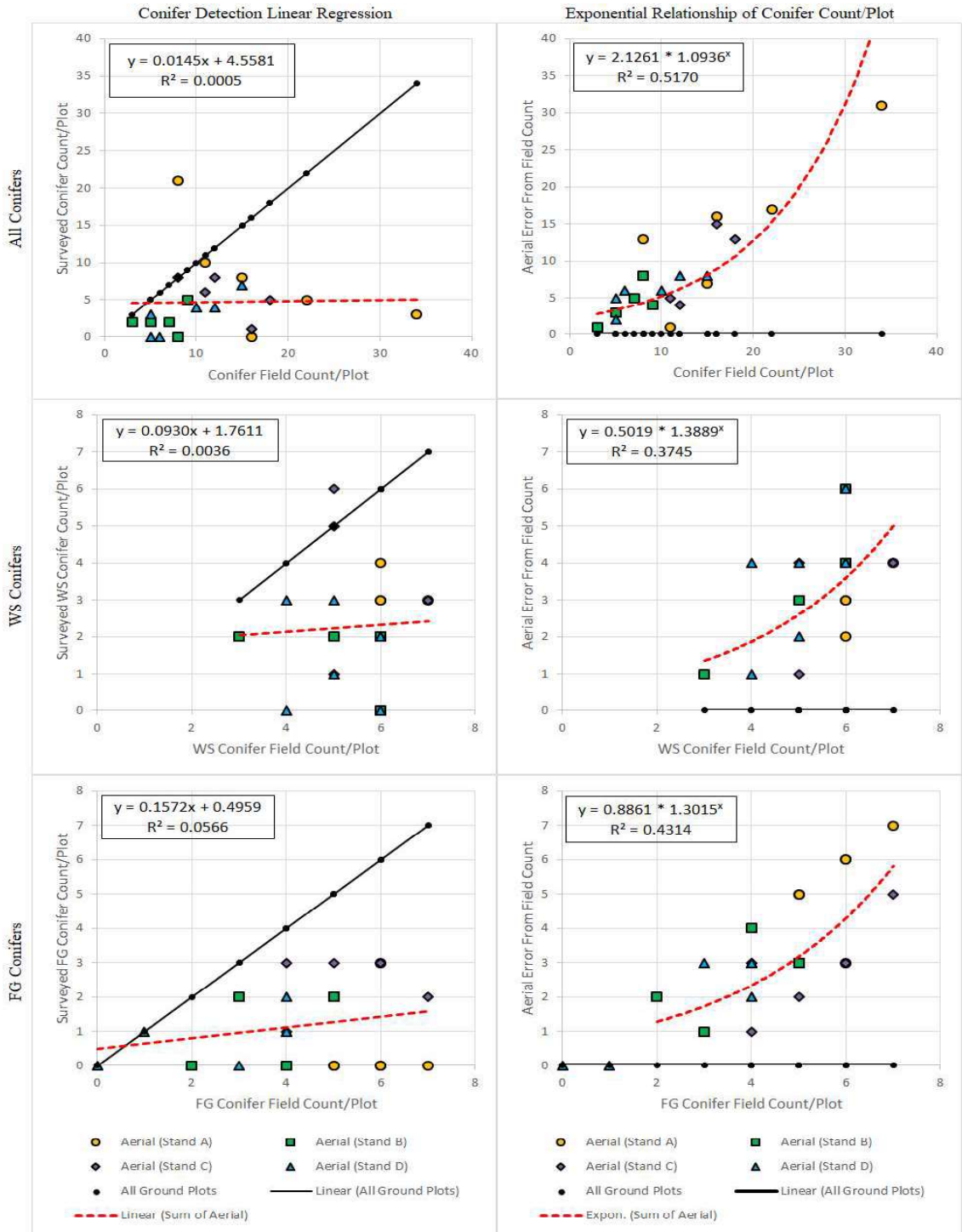


Figure 11. Scatterplots of the aerial and ground surveyed plot data (y-axis) versus the field plot data (x-axis). The conifer detection linear regression (left) indicates no significant correlation between aerial plot survey data and baseline ground plot survey data in any conifer count category (total, WS, and FG). The exponential relationship of conifer count/plot (right) shows the aerial plot survey conifer count error increases exponentially as actual conifer count increases.

GROUND PLOT AND WALL-TO-WALL SURVEYS

The wall-to-wall aerial survey results calculated by the Tree Count algorithm in Table 9 represent the total conifers, WS conifers, and FG conifers for each stand.

Table 9. Sum of conifer count data from aerial wall-to-wall surveys.

Stand ID	Stand Area (ha)	Total Conifer Count	WS Conifer Count	FG Conifer Count
A	5.7	7206	2117	699
B	2.8	2000	849	722
C	5.3	5826	2142	1814
D	6.3	5327	1708	1078

Based on stand area, the wall-to-wall survey data was used to determine the SPH for all conifers, WS conifers, and FG conifers in each entire stand (Table 10). The wall-to-wall conifer count results show a similar pattern to the aerial plot results. All three categories of conifer counts (total, WS, and FG) are underrepresented compared to the baseline ground plot data. The Total Conifers category of each stand ranged from 39% to 56% accuracy with the highest mean accuracy of 47%. The WS Conifers category ranged from 27% to 36% accuracy and a mean accuracy of 32%. The FG Conifers category ranged from 11% to 34% accuracy with the lowest mean accuracy of 28%.

Table 10. Conifer count data and accuracy comparison between ground plot survey and aerial wall-to-wall survey methods.

Stand ID	Ground Survey Sample Size (%)	Aerial Survey Sample Size (%)	Total Conifer Mean			WS Conifer Mean			FG Conifer Mean		
			Ground Plot Survey SPH	Aerial Wall-to-Wall Survey		Ground Plot Survey SPH	Aerial Wall-to-Wall Survey		Ground Plot Survey SPH	Aerial Wall-to-Wall Survey	
				SPH	Accuracy		SPH	Accuracy		SPH	Accuracy
A	0.09%	100%	3533	1369	39%	1200	402	34%	1167	133	11%
B	0.18%	100%	1280	720	56%	1040	306	29%	760	260	34%
C	0.09%	100%	2600	1138	44%	1160	419	36%	1040	354	34%
D	0.08%	100%	1767	846	48%	1000	271	27%	533	172	32%
Mean			2295	1018	47%	1100	350	32%	875	230	28%

The ground plot and aerial wall-to-wall survey SPH and LCL for the three conifer count categories are compared in Table 11.

Table 11. Stand conifer data calculated from ground plot and aerial wall-to-wall survey results.

Stand ID	Total Conifers				WS Conifers				FG Conifers			
	Ground Plot		Aerial Wall-to-Wall		Ground Plot		Aerial Wall-to-Wall		Ground Plot		Aerial Wall-to-Wall	
	Mean (SPH)	LCL (SPH)	Mean (SPH)	LCL (SPH)	Mean (SPH)	LCL (SPH)	Mean (SPH)	LCL (SPH)	Mean (SPH)	LCL (SPH)	Mean (SPH)	LCL (SPH)
A	3533	2002	1369	1369	1200	1100	402	402	1167	1048	133	133
B	1280	821	720	720	1040	791	306	306	760	511	260	260
C	2600	1837	1138	1138	1160	954	419	419	1040	898	354	354
D	1767	1081	846	846	1000	853	271	271	533	245	172	172
Mean	2295	1435	1018	1018	1100	925	350	350	875	676	230	230

The relationships between the wall-to-wall survey results and the baseline ground plot results are represented in Figure 12. The resulting SPH of the aerial wall-to-wall surveys are not significantly correlated (p -value < 0.1) to the ground plot surveys in any conifer count category (total, WS, and FG). Based on linear regression, the WS

conifer count has the highest correlation to plot data, while the FG conifer count has the lowest correlation to plot data.

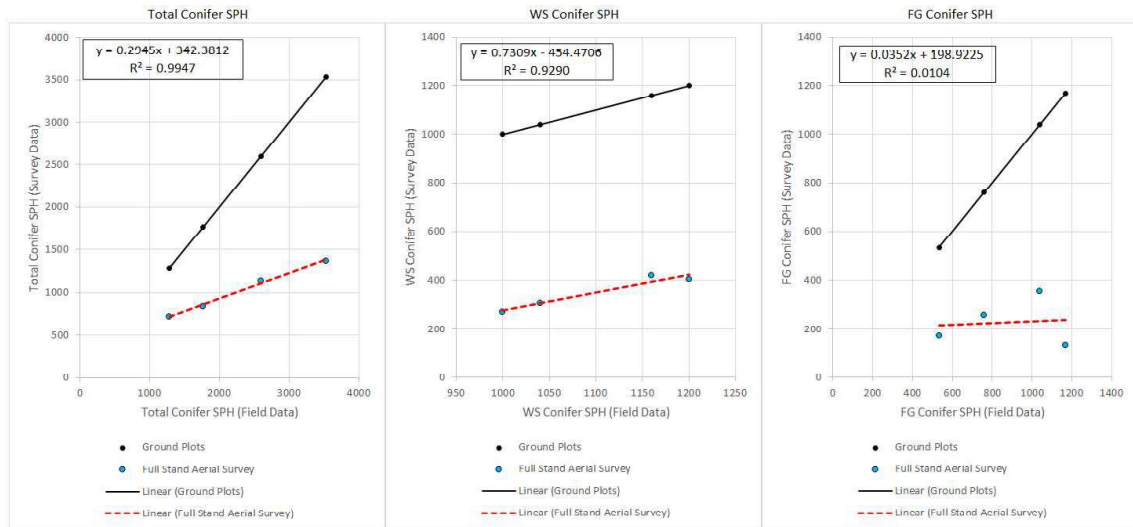


Figure 12. Scatterplots of the surveyed wall-to-wall & ground plot results (y-axis) versus the field plot data (x-axis).

Conifer count accuracy between the two aerial methods were also examined for potential stand characteristics and/or flight parameter correlations. However, the conifer count accuracy between aerial survey methods were highly variable, and no correlation was identified.

TIME AND EFFICIENCY

Ground Plot Surveys

The 22 ground plots in the four stands took a total of 2.2 work-hours to survey with a survey area mean production rate of 0.05 hectares per hour (ha/h). Table 12 represents the summarized ground plot time data. For the purpose of this study, “work-hours” are considered to be hours requiring paid employee compensation. This category is limited to ground plot survey time and aerial flight time only, and tallied separately from computer processing times since processing time does not require active supervision and is significantly less costly. Net survey time includes all survey steps, including survey time (work-hours) and applicable processing time.

Table 12. Ground plot survey time summary.

Stand ID	Stand Area (ha)	# Plots	Net Plot Area (ha)	Survey Time (h)	Survey Production Rate (ha/h)
A	5.7	6	0.030	0.6	0.05
B	2.8	5	0.025	0.5	0.05
C	5.3	5	0.025	0.6	0.04
D	6.3	6	0.030	0.5	0.06

Aerial Plot Surveys

The aerial plot survey method produced all results after 0.7 hours of flight time and 41.5 hours of computer processing time, equating to a net survey time of 42.2 hours, a mean survey time of 10.6 hours, and a mean production rate of 0.003 ha/h (Table 13).

The 0.7 work-hours equates to a mean field-production rate of 0.17 ha/h. The same flight data was used for both the aerial plot survey and wall-to-wall survey. If separate flights were flown for the aerial plot and wall-to-wall surveys, the flight time would have been similar, but the Pix4D processing time would likely have been significantly less.

Table 13. Aerial plot survey time summary.

Stand ID	Area (ha)	# Plots	Net Plot Area (ha)	Flight Time (h)	Pix4D Processing Time (h)	QGIS Plots Processing Time (h)	Net Survey		Work-Hour	
							Time (h)	Production (ha/h)	Time (h)	Production (ha/h)
A	5.7	6	0.030	0.2	7.4	0.1	7.7	0.004	0.2	0.15
B	2.8	5	0.025	0.1	4.4	0.1	4.6	0.005	0.1	0.25
C	5.3	5	0.025	0.2	19.0	0.2	19.4	0.001	0.2	0.13
D	6.3	6	0.030	0.2	10.2	0.1	10.5	0.003	0.2	0.15

Aerial Wall-to-Wall Surveys

The aerial wall-to-wall survey method produced full results after 0.7 hours of flight time and 44.0 hours of computer processing time, equating to a net survey time of 44.7 hours, a mean survey time of 11.2 hours, and a mean production rate of 0.5 ha/h (Table 14). The 0.7 work-hours equates to a mean field-production rate of 28.6 ha/h.

Table 14. Aerial wall-to-wall survey time summary.

Stand ID	Area (ha)	Flight Time (h)	Pix4D Processing Time (h)	QGIS Processing Time (h)	Net Survey		Work-Hour	
					Time (h)	Production (ha/h)	Time (h)	Production (ha/h)
A	5.7	0.2	7.4	0.8	8.4	0.7	0.2	28.5
B	2.8	0.1	4.4	0.2	4.7	0.6	0.1	28.0
C	5.3	0.2	19.0	1.3	20.5	0.3	0.2	26.5
D	6.3	0.2	10.2	0.7	11.1	0.6	0.2	31.5

TIME AND EFFICIENCY COMPARISON

The time and efficiency results for the three survey methods are summarized in Table 15.

Table 15. Time and production rates for the three survey methods (ground plot, aerial plot, and aerial wall-to-wall).

Stand ID	Ground Plot		Aerial Plot				Aerial Wall-to-Wall			
	Time (h)	Production (ha/h)	Net Survey		Work-Hour		Net Survey		Work-Hour	
			Time (h)	Production (ha/h)	Time (h)	Production (ha/h)	Time (h)	Production (ha/h)	Time (h)	Production (ha/h)
A	0.6	0.05	7.7	0.004	0.2	0.15	8.4	0.68	0.2	28.5
B	0.5	0.05	4.6	0.005	0.1	0.25	4.7	0.60	0.1	28.0
C	0.6	0.04	19.4	0.001	0.2	0.13	20.5	0.26	0.2	26.5
D	0.5	0.06	10.5	0.003	0.2	0.15	11.1	0.57	0.2	31.5
Mean	0.6	0.05	10.6	0.003	0.2	0.17	11.2	0.53	0.2	28.6

Net Efficiency and Accuracy

Based on the production rate values in Table 15 (above) and the mean accuracy of the three conifer count categories within each stand, the net efficiency and accuracy of each survey type is compared to the ground plot survey values in Table 16. As the net production rates include computer processing time for the aerial surveys, the efficiency rates vary widely. Compared to the mean ground plot survey production rate of 0.05 ha/h, the mean aerial plot survey production rate of 0.003 ha/h was 93% less efficient at generating conifer count results at a mean accuracy of 37%. A similar comparison

between the mean ground plot survey production rate and the mean aerial wall-to-wall survey production rate of 0.53 ha/h was 942% more efficient at producing conifer count results at a mean accuracy of 37%. The vast majority of inefficiencies observed in the aerial method were the result of slow computer processing speeds which can be easily improved by upgrading computer hardware. Technological advancements in processing power and data management systems are expected to significantly increase the efficiency of this step in the near future.

Table 16. Net efficiency and accuracy comparison of the two aerial survey methods to the ground plot data which acts as the control data set.

Stand ID	Ground Plot (Baseline)			Aerial Plot			Aerial Wall-to-Wall		
	Production Rate (ha/h)	Efficiency (%)	Accuracy (%)	Production Rate (ha/h)	Efficiency (%)	Accuracy (%)	Production Rate (ha/h)	Efficiency (%)	Accuracy (%)
A	0.05	100%	100%	0.004	8%	32%	0.68	1357%	28%
B	0.05	100%	100%	0.005	11%	32%	0.60	1191%	40%
C	0.04	100%	100%	0.001	3%	50%	0.26	620%	38%
D	0.06	100%	100%	0.003	5%	32%	0.57	946%	36%
Mean	0.05	100%	100%	0.003	7%	37%	0.53	1042%	36%

Work-Hour Efficiency and Accuracy

While the net survey efficiency is an important factor to consider, the work-hour production rate is a more relevant measure of efficiency between the three survey types. From a cost perspective, the field production rate is the most important variable since the computer processing costs for aerial surveys is negligible, and do not require hourly compensation for active work. Similarly, multiple survey datasets can be processed

simultaneously with appropriate hardware and software. The comparison of work-hour efficiency and accuracy rates between the three survey methods is summarized in Table 17. Compared to the mean ground plot survey production rate of 0.05 ha/h, the mean work-hour aerial survey production rate of 0.17 ha/h was 235% more efficient at generating conifer count results at a mean accuracy of 37%. The mean work-hour production rate for the aerial wall-to-wall survey method (28.6 ha/h) was 56677% more efficient at generating conifer count results at a mean accuracy of 37%. The stands used in this study were relatively small due to time constraints, but the aerial field data collection efficiency rate is expected to increase with stand survey size due to fatigue and in-stand travel time differences between survey methods.

Table 17. Work-hour efficiency and accuracy comparison for the three survey methods (ground plot, aerial plot, and aerial wall-to-wall).

Stand ID	Ground Plot (Baseline)			Aerial Plot			Aerial Wall-to-Wall		
	Production Rate (ha/h)	Efficiency (%)	Accuracy (%)	Production Rate (ha/h)	Efficiency (%)	Accuracy (%)	Production Rate (ha/h)	Efficiency (%)	Accuracy (%)
A	0.05	100%	100%	0.15	300%	32%	28.5	57000%	28%
B	0.05	100%	100%	0.25	500%	32%	28.0	56000%	40%
C	0.04	100%	100%	0.13	300%	50%	26.5	63600%	38%
D	0.06	100%	100%	0.15	250%	32%	31.5	52500%	36%
Mean	0.05	100%	100%	0.17	335%	37%	28.6	56777%	36%

DISCUSSION

The three hypotheses of this study were designed as a linear workflow to determine the feasibility of using DAP point cloud data to efficiently determine the stocking status of forest openings. The complete conifer count results from the four stands surveyed indicate that the total, WS, and FG conifer counts can be automatically detected using DAP point cloud processing algorithms, proving H_1 to be true. This can be accomplished using simple UAV-derived DSM, DTM, and orthomosaic stand data.

The conifer count results and comparison to the ground plot survey data indicate that there is a significant difference (p -value < 0.1) between the total stem counts of the ground plot surveys compared to those of the UAV surveys, proving H_2 to be false. Despite several weak correlations between the ground plot results and UAV results, the methods used in this study demonstrate that low-cost UAV-collected silviculture data is not capable of accurately determining the stocking status of forest stands using automated detection algorithms. Compared to similar studies in mature plantations and simple forest openings with successful results, the stands surveyed in this study were relatively complex. Natural conifer regeneration of various ages and heights were observed among planted conifers in each surveyed stand, as well as variable densities of deciduous and brush species. Due to the complicated stand structures, the Tree Count algorithm struggled to identify conifer germinants and delineate conifers based on RGB reflectance. Assisted by CHM values, the algorithm was able to detect established

conifers with well-defined crowns, but height data was likely skewed by the DTM which smoothed the herbaceous brush and small trees into the model.

Despite insufficient aerial survey accuracy results, the efficiency of each survey method is considered for H_3 . The net efficiency including all computer processing time was 93% less efficient and 942% more efficient for the aerial plot survey method and the aerial wall-to-wall survey method respectively. When only considering work-hour efficiency, the aerial plot survey method was 235% more efficient and the aerial wall-to-wall survey method was 56677% more efficient. Therefore, H_3 is proven to be false for the net aerial plot survey efficiency, but true for the work-hour aerial plot survey efficiency. Given the high efficiencies for both the net and work-hour aerial wall-to-wall survey method, H_3 is proven to be true for this method.

The aerial data collection methods used in this study were intended to closely emulate the real-world constraints of traditional silviculture field work, including production targets and acceptable data quality limits. Considering the high efficiency rates and low accuracy rates of aerial surveys, survey flight time can be increased to improve the quality of the data collected. As a result of longer flight times, flight parameters can be improved by decreasing altitude, increasing image overlap, and increasing look angles. These factors, along with others affecting survey accuracy, are further discussed below.

SOURCES OF LINEAR ERROR

Low Point Cloud Density

As a result of the relatively high flight altitude and manually-flown single-grid flight surveys, the point clouds produced by Pix4D along with the resulting CHMs had considerable patches of blind spots where the imagery did not capture enough detail to accurately model elevation using SFM (Figure 13). The most important factor in conifer identification is a well-defined CHM as the algorithm uses CHM peaks to produce stem counts. Similarly, clumped conifers will be more accurately detected by achieving higher resolution point cloud data (Figure 14). It is estimated that patches of low point cloud density contributed to 5% of the accuracy errors encountered in this study. To increase aerial conifer count accuracy, pre-programmed double-grid flight missions should be flown as low as consistently possible.

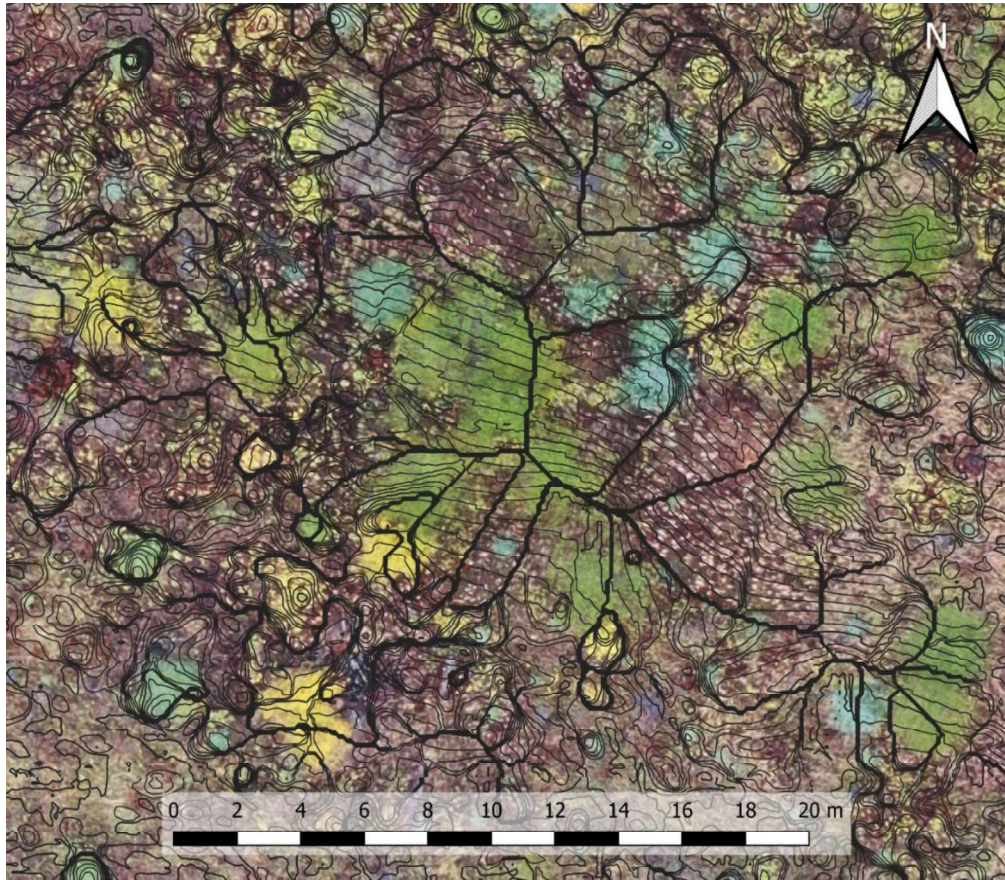


Figure 13. CHM contours showing a blind spot example with conifer height errors.



Figure 14. Low resolution point cloud mesh showing poorly defined conifer clump.

GPS-Related CHM Errors

The limited GPS accuracy in the DJI Mavic 2 likely contributed to some minor elevation errors during the SfM point cloud development process. Further studies may be required to determine the significance of this source of error, which can be reduced by establishing GCPs during aerial surveys. Given elevation data is triangulated from GPS location and image features, GPS-related CHM errors likely increase as altitude AGL decreases. Since aerial surveys in this study were flown at relatively high altitudes, the GPS-related CHM errors are probably negligible. Future high resolution aerial plot surveys flown at low altitudes should require the use of GCPs for accurate elevation data.

SOURCES OF EXPONENTIAL ERROR

Camera Angle

Aerial imagery was collected using a nadir camera angle which is only able to collect vegetation data along the top surfaces of features (tree crowns). Any conifer saplings or germinants growing below another conifer is undetectable with nadir RGB imagery (Figure 15). Detection can be improved by gathering oblique imagery to supplement the dataset, however there will always be some degree of error caused by this method (Nesbit and Hugenholtz 2019). Depending on the species composition and

structure, this can significantly affect conifer count results and stand stocking status. It is estimated that camera angle factors contributed to 30% of the accuracy errors encountered in this study. Given enough baseline data, a correlation between stand characteristics and percent conifer count error due to camera angle could be developed. The tendency for camera angle to under-detect conifers has a negative effect on the upper confidence limits for aerial surveys, but has no effect on the lower confidence limits. Aerial conifer count accuracy can likely be marginally improved by supplementing nadir imagery with oblique imagery. Recommended camera angles generally range between 10 - 45° for supplemental oblique imagery to improve SfM point cloud development (Nesbit and Hugenholtz 2019).

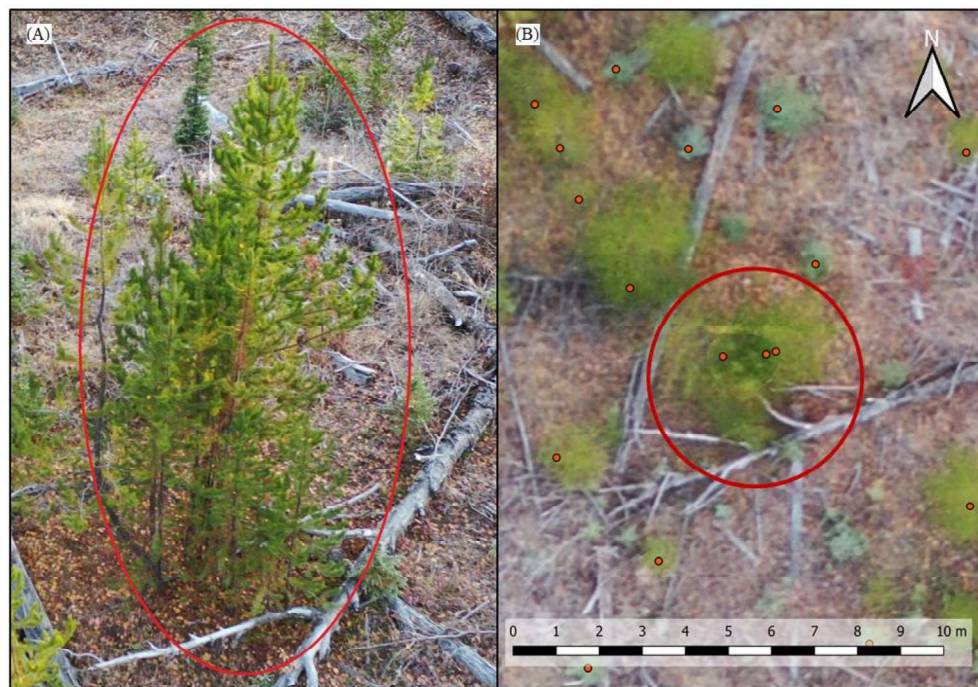


Figure 15. Clumped Lodgepole pine growing below/adjacent to a central dominant stem. (A): Oblique photo showing >7 stems in clump. (B): Orthomosaic of the same clump displaying underrepresented conifer count results from the Tree Count algorithm as red dots.

DTM Creation

The DTMs created in Pix4D are based on factors including DTM resolution, elevation, and point cloud structure which are smoothed to represent the best estimate of the true terrain elevation. As discussed by Goodbody et al. (2017) and Hartley et al. (2020), DTMs are often unable to accurately represent true elevation in stands with complex forest structure such as dense herbaceous brush because the DAP point cloud is unable to penetrate the brush layer. As a result, the brush layer is assumed to be the bare terrain elevation, which skews CHM data and prevents all conifers shorter than the brush from being detected. It is estimated that the majority of small conifers <0.3m tall were undetected by the Tree Count algorithm due to DTM creation errors, which likely equates to 40% of the accuracy errors encountered in this study. The ability to reduce this error in complex stands is limited while solely relying on DAP point clouds. Without LiDAR to penetrate the brush layer, it is recommended that stands with complex structures should not be surveyed for tree height using aerial survey methods in combination solely with current automated height classification algorithms.

Pixel Size

Another major contributor of exponential conifer count error is caused by a relatively low orthomosaic resolution which is unable to detect small conifers. The average pixel resolution in this study (2.83 cm/px) is too low for the Tree Count

algorithm to successfully delineate most conifers < 0.3 m tall (Figure 16). Conifer germinants can be as small as one pixel, making them virtually undetectable in the datasets used for this study. This error is exponential because conifer density generally increases as conifer size decreases. Conifer germinants can often occur at >100 /plot, while large established conifers (>1 m tall) are generally regularly spaced and occur at lower densities within plots. It is estimated that pixel size contributed to 25% of the accuracy errors encountered in this study. To reduce errors associated with pixel size, UAVs should be equipped with high resolution cameras and flown as low as consistently possible.

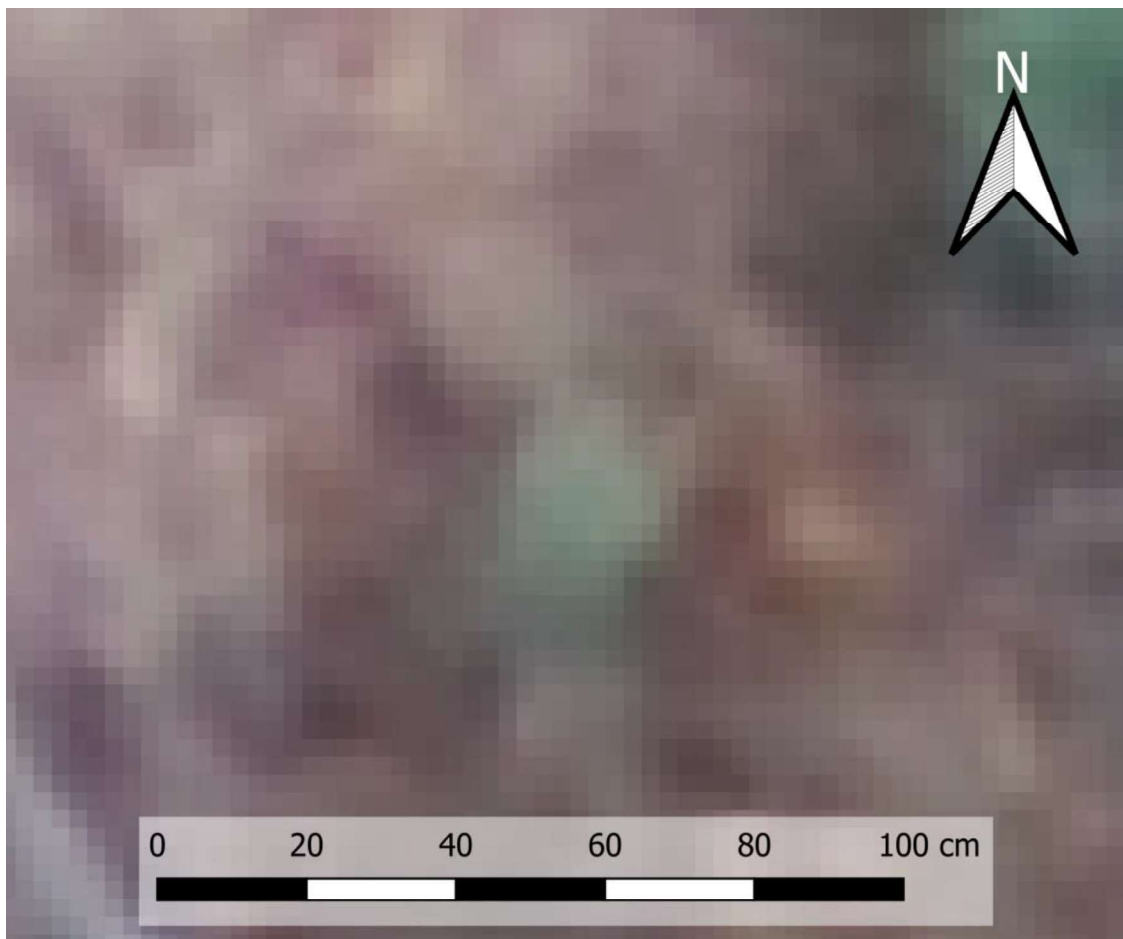


Figure 16. An undetected spruce tree that was 20 cm wide showing relative pixel size.

FUTURE DEVELOPMENT

To further improve the automated aspect of low-cost ITD, tree height measurements, and other silviculture metrics, the following approaches are recommended based on the results of this study;

To ensure accurate CHM data for the entire regeneration stage of a stand, a DTM should be produced using ALS immediately prior to tree planting. Despite the relatively high initial cost, all subsequent aerial surveys can be conducted with DAP point clouds. The ALS-derived DTM can be compared to the most recent DAP-derived DSM to produce an accurate CHM for height and growth rate calculations. Given enough stand data across a landscape, this will allow for more accurate estimations for many metrics including time to reach FG status, and growth and yield modeling.

The automated detection algorithm process used in this study, along with other common ITD processes, rely on detection methods designed for other purposes including hydraulic and topographical modeling. Specifically-designed ITD algorithms are being developed (Nitoslawski et al. 2021), but are not yet widely available at low costs. With more research and development expected in the near future, the accuracy of specifically-designed ITD algorithm tools are expected to significantly improve.

Finally, to allow for better conifer delineation within tree clumps, identification of various conifer species within a stand, and detection of stand health, it is recommended to supplement RGB imagery with low-cost multispectral sensors. This

can be as simple as modifying a RGB sensor to capture red-edge, or as complex as capturing data with a multispectral system.

BALANCING ACCURACY AND EFFICIENCY

For low-cost aerial survey and automated tree detection methods to be widely used in the industry, the stocking status data (SPH and LCL) must be statistically significant and regularly tested for accuracy. At minimum, automatic workflows need to be able to delineate trees >30 cm tall based on their crown peaks. To accomplish this, the results of Castilla et al. (2020) suggest that a GSD of 0.35 cm or less is required (Figure 17). Using consumer-grade UAVs such as the DJI Mavic 2, flights must be consistently flown at approximately 15 m AGL to achieve a GSD of 0.35 cm. Flying double-grid flight patterns at this altitude (and assuming no obstacles), UAV flight time and computer processing time is estimated to be at least 10x more time consuming than the methods used in this study. Compared to the traditional ground plot survey method production rate of 0.05 ha/hour, the aerial survey methods are expected to be marginally more efficient. The net production rate for either survey method is estimated be 0.053 ha/hour, while the work-hour production rate for either survey method is estimated to be 2.8 ha/hour. It is important to note that this scenario considers refined aerial plot survey methodology, reducing relative flight time and equating to a similar production rate to that of the wall-to-wall survey method. Despite direct comparisons of both aerial methods showing slightly higher production rates, the traditional ground plot survey

method includes an acceptable expansion factor of 200 to determine stocking status. Taking this into account, the traditional ground plot method achieved a representative production rate of 9.1 ha/hour. With all aerial method factors considered, current technology and workflows limit low-cost aerial data collection methods from exceeding the accuracy and/or efficiency of traditional ground plot surveys actively used in the industry. Aerial tree detection accuracy will likely always be lower than traditional ground plot tree counts, making aerial plot data statistically difficult to equate. It's likely that high resolution aerial wall-to-wall survey data will be able produce statistically significant determinations of stocking status, but higher resolution sensors must be used to collect data more efficiently. From a cost perspective for licensees and silviculture contractors, traditional ground plot surveys are still the most accurate and efficient data collection method compared to low-cost aerial data collection methods. However, the use of industrial-grade high resolution RGB sensors (>40 MP) combined with the refined methodologies discussed earlier may produce an acceptable level of accuracy with significantly improved efficiency.

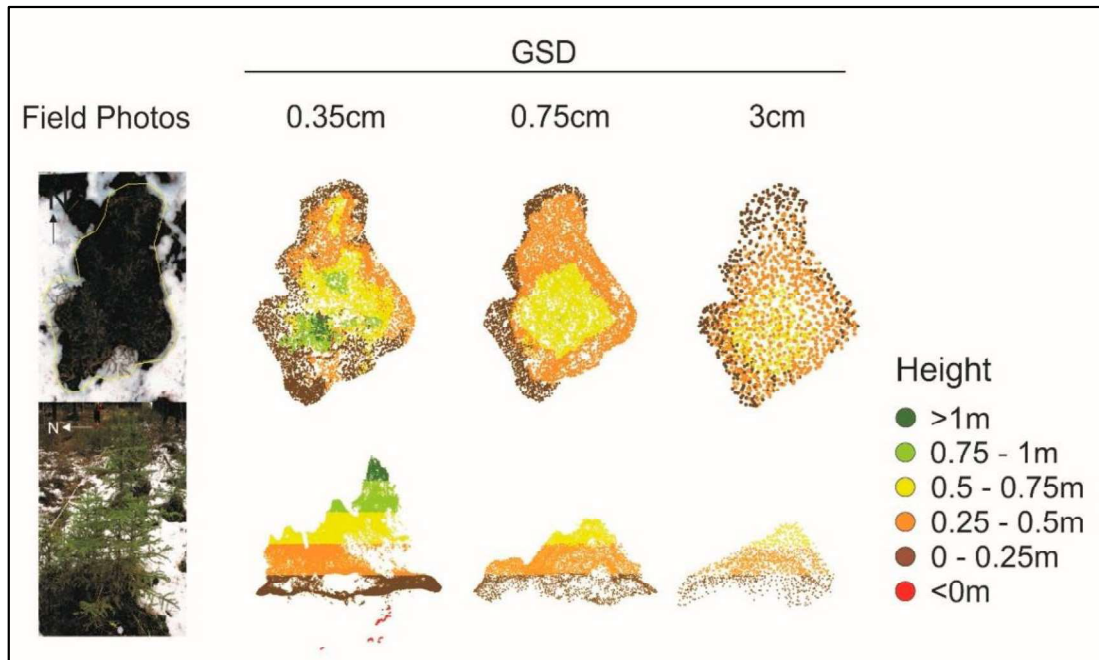


Figure 17. Relative point cloud densities, 3D reconstruction details, and height estimation for a cluster of spruce trees. Source: Castilla et al. (2020).

CONCLUSION

The intent of this study was to determine the capabilities and limitations of low-cost UAV-collected silviculture data. This was accomplished by evaluating the feasibility of using UAV RGB imagery and automatic tree detection to determine the silviculture stand stocking status of four regenerating forest stands. Although similar studies accomplished statistically significant tree count correlations in simple stand structures, this study attempted similar methods in complex stand structures common in BC silviculture. This is important because it highlights the real-world feasibility of low-cost aerial survey methods, and contributes to the development of resilient tree detection algorithms. Despite relatively low conifer count accuracy achieved across the four stands, aerial survey methods have the potential to significantly increase survey efficiency and decrease labour costs by supplementing ground-based survey efforts. In addition, five sources of conifer count accuracy errors were identified and mitigation measures discussed.

The findings of this study have identified several opportunities for further research. The relationship between various categories of stand structures and conifer count accuracy needs to be better understood. Similarly, in order to fully determine the silviculture status of a stand, the accuracy for DAP point clouds to model deciduous trees must be determined. Most importantly, resilient workflows for UAV surveys must be further developed to ensure consistently accurate measurements across variable stand structures.

LITERATURE CITED

- Asner, G.P., R.E. Martin, C.B. Anderson and D.E. Knapp. 2015. Quantifying forest canopy traits: Imaging spectroscopy versus field survey. *Remote Sensing of Environment*, 158, 15–27. <https://doi.org/10.1016/j.rse.2014.11.011>.
- B.C. Ministry of Forests. 2000. Establishment to free growing guidebook. Kamloops Forest Region. Rev. ed., Version 2.2. For. Prac. Br., B.C. Min. For., Victoria, B.C. Forest Practices Code of British Columbia Guidebook. 169pp.
- Carr, J.C. and J.B. Snyder. 2018. Individual tree segmentation from a leaf-off photogrammetric point cloud. *International Journal of Remote Sensing*, 39(15-16), 5195–5210. <https://doi.org/10.1080/01431161.2018.1434330>.
- Castilla, G., M. Filiatrault, G.J. McDermid and M. Gartrell. 2020. Estimating individual conifer seedling height using drone-based image point clouds. *Forests*, 11(9):924–946. <https://doi.org/10.3390/f11090924>.
- Chadwick, A.J., T.R.H. Goodbody, N.C. Coops, A. Hervieux, C.W. Bater, L.A. Martens, B. White and D. Roeser. 2020. Automatic Delineation and Height

Measurement of Regenerating Conifer Crowns under Leaf-Off Conditions Using UAV Imagery. *Remote Sensing* (Basel, Switzerland), 12(24), 4104.
<https://doi.org/10.3390/rs12244104>.

Chen, S., D. Liang, B. Ying, W. Zhu, G. Zhou and Y. Wang. 2021. Assessment of an improved individual tree detection method based on local-maximum algorithm from unmanned aerial vehicle RGB imagery in overlapping canopy mountain forests. *International Journal of Remote Sensing* 42(1):106–125.
<https://doi.org/10.1080/01431161.2020.1809024>.

Chen, S., G.J. McDermid, G. Castilla and J. Linke. 2017. Measuring vegetation height in linear disturbances in the boreal forest with UAV photogrammetry. *Remote Sensing* 9(12):1257–1278. <https://doi.org/10.3390/rs9121257>.

Dainelli, R., P. Toscano, S.F. Di Gennaro and A. Matese. 2021. Recent Advances in Unmanned Aerial Vehicles Forest Remote Sensing - A Systematic Review. Part II: Research Applications. *Forests* 2021, 12, 397. <https://doi.org/10.3390/f12040397>.

Damer, H. 2019. TreeCount QGIS Plugin (Version 1.0) [Software].

DJI. 2022. Mavic 2. <https://www.dji.com/ca/mavic-2/>. March 11, 2022.

Dvořák, P., J. Müllerová, T. Bartaloš and J. Brůna. 2015. Unmanned aerial vehicles for alien plant species detection and monitoring. *The International Archives of the Photogrammetry, Remote Sensing and Spatial Information Sciences*, XL-1/W4:83–90. <https://doi.org/10.5194/isprsarchives-XL-1-W4-83-2015>.

Esri. 2022. "World Imagery" [basemap]. Scale Not Given. <https://www.arcgis.com/home/item.html?id=10df2279f9684e4a9f6a7f08febac2a9>. February 7, 2022.

Feduck, C., G. McDermid and G. Castilla. 2018. Detection of coniferous seedlings in UAV imagery. *Forests*, 9(7):432-447. <https://doi.org/10.3390/f9070432>.

Fernandez-Guisuraga, J.M., E. Sanz-Ablanedo, S. Suarez-Seoane and L. Calvo. 2018. Using unmanned aerial vehicles in postfire vegetation survey campaigns through large and heterogeneous areas: Opportunities and challenges. *Sensors* 18(2):586–603. <https://doi.org/10.3390/s18020586>

Fromm, M., M. Schubert, G. Castilla, J. Linke and G. McDermid. 2019. Automated Detection of Conifer Seedlings in Drone Imagery Using Convolutional Neural Networks. *Remote Sensing (Basel, Switzerland)*, 11(21), 2585. <https://doi.org/10.3390/rs11212585>.

[FRPA] Forest and Ranges Practices Act, SBC. 2002, c. 69.

Gallardo-Salazar, J.L. and M. Pompa-Garcia. 2020. Detecting Individual Tree Attributes and Multispectral Indices Using Unmanned Aerial Vehicles: Applications in a Pine Clonal Orchard. *Remote Sensing* (Basel, Switzerland), 12(24), 4144–4166. <https://doi.org/10.3390/rs12244144>.

Goldbergs, G., S.W. Maier, S.R. Levick and A. Edwards. 2018. Efficiency of Individual Tree Detection Approaches Based on Light-Weight and Low-Cost UAS Imagery in Australian Savannas. *Remote Sensing* (Basel, Switzerland), 10(2), 161–180. <https://doi.org/10.3390/rs10020161>.

Goodbody, T.R.H., N.C. Coops, P.L. Marshall, P. Tompalski and P. Crawford. 2017. Unmanned aerial systems for precision forest inventory purposes: A review and case study. *Forestry Chronicle*, 93(1), 71–81. <https://doi.org/10.5558/tfc2017-012>.

Goodbody, T.R.H., N.C. Coops, T. Hermosilla, P. Tompalski and P. Crawford. 2018. Assessing the status of forest regeneration using digital aerial photogrammetry and unmanned aerial systems. *International Journal of Remote Sensing* 39(15-16):5246–5264. <https://doi.org/10.1080/01431161.2017.1402387>.

- Haddow, K.A., D.J. King, D.A. Pouliot, D.G. Pitt and F.W. Bell. 2000. Early regeneration conifer identification and competition cover assessment using airborne digital camera imagery. *Forestry Chronicle* 76(6):915–928. <https://doi.org/10.5558/tfc76915-6>.
- Hartley, R.J.L., E.M. Leonardo, P. Massam, M.S. Watt, H.J. Estarija, L. Wright, N. Melia and G.D. Pearse. 2020. An Assessment of High-Density UAV Point Clouds for the Measurement of Young Forestry Trials. *Remote Sensing (Basel, Switzerland)*, 12(24), 4039–4059. <https://doi.org/10.3390/rs12244039>.
- Hird, J.N., A. Montaghi, G.J. McDermid, J. Kariyeva, B.J. Moorman, S.E. Nielsen and A.C.S. McIntosh. 2017. Use of unmanned aerial vehicles for monitoring recovery of forest vegetation on petroleum well sites. *Remote Sensing* 9(5):413–433. <https://doi.org/10.3390/rs9050413>.
- Iglhaut, J., C. Cabo, S. Puliti, L. Piermattei, J. O'Connor and J. Rosette. 2019. Structure from Motion Photogrammetry in Forestry: a Review. *Current Forestry Reports*, 5(3), 155–168. <https://doi.org/10.1007/s40725-019-00094-3>.
- King, D.J. 2000. Airborne remote sensing in forestry: Sensors, analysis and applications. *Forestry Chronicle*, 76(6), 859–876. <https://doi.org/10.5558/tfc76859-6>.

Liang, X., Y. Wang, J. Pyörälä, M. Lehtomäki, X. Yu, H. Kaartinen, A. Kukko, E. Honkavaara, A.E.I. Issaoui, O. Nevalainen, M. Vaaja, J.P. Virtanen, M. Katoh and S. Deng. 2019. Forest in situ observations using unmanned aerial vehicle as an alternative of terrestrial measurements. *Forest Ecosystems* 6(1):1–16.
<https://doi.org/10.1186/s40663-019-0173-3>.

Liu, J., Z. Feng, L. Yang, A. Mannan, T.U. Khan, Z. Zhao and Z. Cheng. 2018. Extraction of Sample Plot Parameters from 3D Point Cloud Reconstruction Based on Combined RTK and CCD Continuous Photography. *Remote Sensing (Basel, Switzerland)*, 10(8), 1299–1321. <https://doi.org/10.3390/rs10081299>.

[MFLNRORD] Ministry of Forests, Lands, Natural Resources Operations and Rural Development. 2018. Forest Stewardship Plans in British Columbia. MFLNRORD. 29pp.

[MFLNRORD] Ministry of Forests, Lands, Natural Resources Operations and Rural Development. 2020. Silviculture Surveys Procedures Manual. MFLNRORD – Resource Practices Branch. 330pp.

Mohan, M., C.A. Silva, C. Klauberg, P. Jat, G. Catts, A. Cardil, A.T. Hudak and M. Dia. 2017. Individual tree detection from unmanned aerial vehicle (UAV) derived

canopy height model in an open canopy mixed conifer forest. *Forests* 8:340-357.
<https://doi.org/10.3390/f8090340>.

Nesbit, P.R. and C.H. Hugenholtz. 2019. Enhancing UAV–SfM 3D Model Accuracy in High-Relief Landscapes by Incorporating Oblique Images. *Remote Sensing* (Basel, Switzerland), 11(3), 239. <https://doi.org/10.3390/rs11030239>.

Nevalainen, O., E. Honkavaara, S. Tuominen, N. Viljanen, T. Hakala, X. Yu, J. Hyypä, H. Saari, I. Pölönen, N. Imai and A. Tommaselli. 2017. Individual Tree Detection and Classification with UAV-Based Photogrammetric Point Clouds and Hyperspectral Imaging. *Remote Sensing* (Basel, Switzerland), 9(3), 185–219.
<https://doi.org/10.3390/rs9030185>.

Nitoslawski, S.A., K. Wong-Stevens, J.W.N Steenberg, K. Witherspoon, L. Nesbitt and C.C. Konijnendijk van den Bosch. 2021. The digital forest: Mapping a decade of knowledge on technological applications for forest ecosystems. *Earth's Future*: e2021EF002123. <https://doi.org/10.1029/2021EF002123>.

Pitt, D.G., U. Runesson and F.W. Bell. 2000. Application of large- and medium-scale aerial photographs to forest vegetation management: A case study. *Forestry Chronicle*, 76(6), 903–913. <https://doi.org/10.5558/tfc76903-6>.

Pouliot, D.A., D.J. King, F.W. Bell and D.G. Pitt. 2002. Automated tree crown detection and delineation in high-resolution digital camera imagery of coniferous forest regeneration. *Remote Sensing of Environment* 82(2):322–334.
[https://doi.org/10.1016/S0034-4257\(02\)00050-0](https://doi.org/10.1016/S0034-4257(02)00050-0).

Puliti, S., S. Solberg and A. Granhus. 2019. Use of UAV photogrammetric data for estimation of biophysical properties in forest stands under regeneration. *Remote Sensing* 11(3): 233–248. <https://doi.org/10.3390/rs11030233>.

Reid, D.E.B., J. Hagens and D. Wojick. 2019. Evaluating the use of digital aerial photogrammetry for free to grow surveys. Ontario Ministry of Natural Resources and Forestry, Science and Research Branch, Peterborough, ON. Science and Research Technical Report TR-32. 42 p. + appendices.

Röder, M., H. Latifi, S. Hill, J. Wild, M. Svoboda, J. Brůna, M. Macek, M.H. Nováková, E. Gülch and M. Heurich. 2018. Application of optical unmanned aerial vehicle-based imagery for the inventory of natural regeneration and standing deadwood in post-disturbed spruce forests. *International Journal of Remote Sensing* 39(15-16):5288–5309. <https://doi.org/10.1080/01431161.2018.1441568>.

Saarinen, N., M. Vastaranta, R. Näsi, T. Rosnell, T. Hakala, E. Honkavaara, M.A.

Wulder, V. Luoma, A.M.G. Tommaselli, N.N. Imai, E.A.W. Ribeiro, R.B.

Guimarães, M. Holopainen and J. Hyypä. 2018. Assessing Biodiversity in Boreal

Forests with UAV-Based Photogrammetric Point Clouds and Hyperspectral

Imaging. *Remote Sensing* (Basel, Switzerland), 10(2), 338.

<https://doi.org/10.3390/rs10020338>.

Tang, L. and G. Shao. 2015. Drone remote sensing for forestry research and practices.

Journal of Forestry Research, 26(4):791–797. [https://doi.org/10.1007/s11676-015-](https://doi.org/10.1007/s11676-015-0088-y)

0088-y.

Transport Canada. 2020. Getting a drone pilot certificate. Government of Canada.

[https://tc.canada.ca/en/aviation/drone-safety/drone-pilot-licensing/getting-drone-](https://tc.canada.ca/en/aviation/drone-safety/drone-pilot-licensing/getting-drone-pilot-certificate)

pilot-certificate. Nov. 02, 2021.

Vepakomma, U., D. Cormier and N. Thiffault. 2015. Potential of UAV based convergent

photogrammetry in monitoring regeneration standards. *Int. Arch. Photogramm.*

Remote Sens. Spatial Inf. Sci. XL-1-W4:281–285.

<https://doi.org/10.5194/isprsarchives-XL-1-W4-281-2015>.

Zhang, J., J. Hu, J. Lian, Z. Fan, X. Ouyang and W. Ye. 2016. Seeing the forest from drones: Testing the potential of lightweight drones as a tool for long-term forest monitoring. *Biological Conservation* 198:60–69.
<https://doi.org/10.1016/j.biocon.2016.03.027>.

APPENDICES

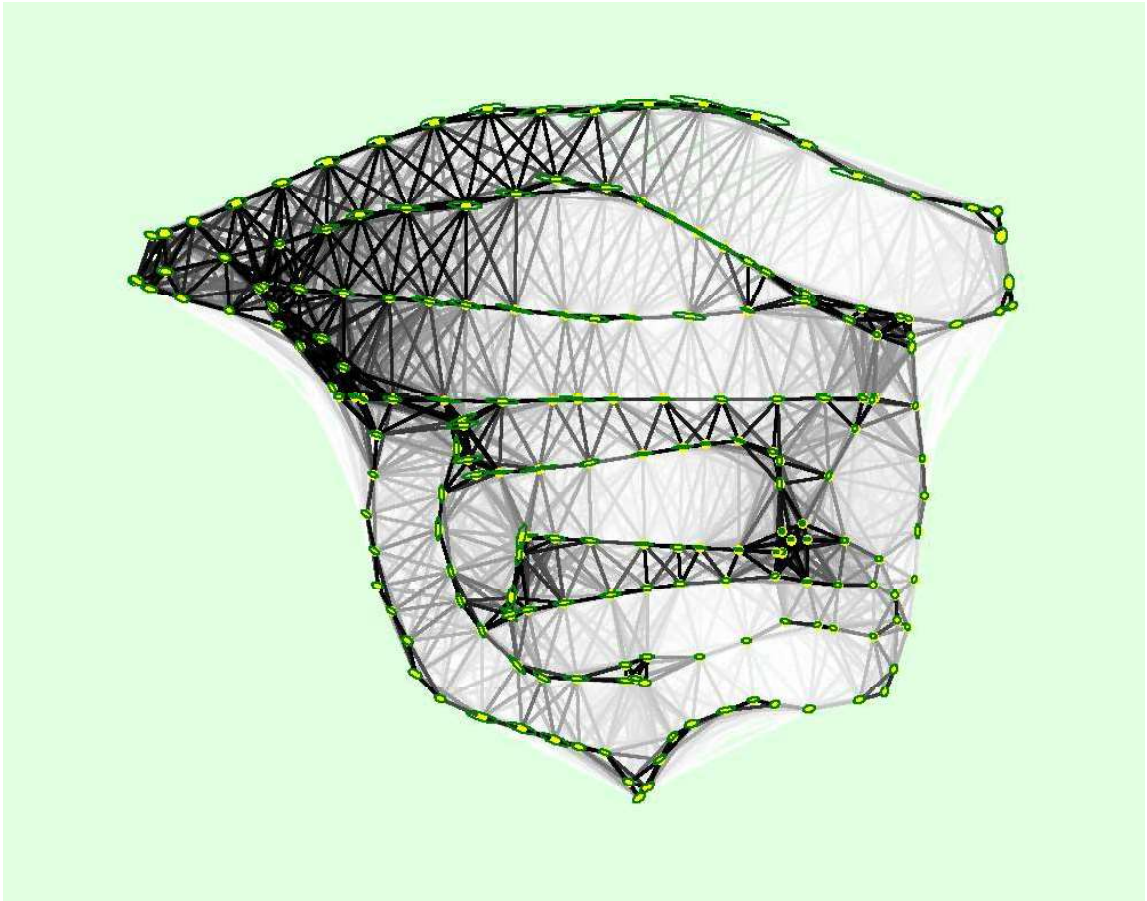
APPENDIX I

RAW CONIFER COUNT RESULTS FOR THE FOUR STANDS SURVEYED

Stand ID	Plot #	Total Conifers			Total WS Conifers			Total FG Conifers		
		Ground Survey	Aerial Survey	Error (%)	Ground Survey	Aerial Survey	Error (%)	Ground Survey	Aerial Survey	Error (%)
A	1	34	3	-91%	6	3	-50%	6	3	-50%
	2	8	21	163%	6	3	-50%	5	0	-100%
	3	16	0	-100%	6	0	-100%	6	0	-100%
	4	15	8	-47%	7	3	-57%	7	0	-100%
	5	22	5	-77%	5	2	-60%	5	0	-100%
	6	11	10	-9%	6	4	-33%	6	0	-100%
	SPH (Plots)	3533	1567	-56%	1200	500	-58%	1167	100	-91%
	SPH (NAR)	N/A	1369	-61%	N/A	402	-67%	N/A	133	-89%
B	1	3	2	-33%	3	2	-33%	3	2	-33%
	2	8	0	-100%	6	0	-100%	2	0	-100%
	3	5	2	-60%	5	2	-60%	5	2	-60%
	4	9	5	-44%	6	2	-67%	4	0	-100%
	5	7	2	-71%	6	2	-67%	5	2	-60%
	SPH (Plots)	1280	440	-66%	1040	320	-69%	760	240	-68%
	SPH (NAR)	N/A	720	-44%	N/A	306	-71%	N/A	260	-66%
C	1	8	8	0%	7	3	-57%	7	2	-71%
	2	12	8	-33%	5	5	0%	4	3	-25%
	3	18	5	-72%	7	3	-57%	6	3	-50%
	4	11	6	-45%	5	6	20%	5	3	-40%
	5	16	1	-94%	5	1	-80%	4	1	-75%
	SPH (Plots)	2600	1120	-57%	1160	720	-38%	1040	480	-54%
	SPH (NAR)	N/A	1138	-56%	N/A	419	-64%	N/A	354	-66%
D	1	5	3	-40%	4	3	-25%	4	2	-50%
	2	10	4	-60%	5	1	-80%	1	1	0%
	3	5	0	-100%	4	0	-100%	0	0	0%
	4	12	4	-67%	6	2	-67%	4	1	-75%
	5	15	7	-53%	5	3	-40%	4	1	-75%
	6	6	0	-100%	6	0	-100%	3	0	-100%
	SPH (Plots)	1767	600	-66%	1000	300	-70%	533	167	-69%
	SPH (NAR)	N/A	846	-52%	N/A	271	-73%	N/A	172	-68%

APPENDIX II

STAND A EXAMPLE OF 2D IMAGERY MATCHES DURING PIX4D
PROCESSING



APPENDIX III

COMPUTER PROCESSING SYSTEM INFORMATION

Hardware	CPU: Intel(R) Core(TM) i5-10300H CPU @2.50GHz RAM: 16GB GPU: Intel(R) UHD Graphics (Driver: 27.20.100.8280), NVIDIA GeForce GTX 1650 Ti (Driver: 27.21.14.5167)
Operating System	Windows 10 Home, 64-bit